




A Spatial–Deep Learning Hybrid Model for Cryptocurrency Pricing and Optimal Trading Strategy Design for Capital Management

Alireza Zamanian¹, Mohammad Aslani^{2,*} and Mahmud Hematfar³



¹ Ph.D. student, Department of Accounting, Bo.c., Islamic Azad University, Borujerd, Iran; 

² Assistant Professor, Department of Accounting, Tu.C., Islamic Azad University, Tuyserkan, Iran; 

³ Associate Professor, Department of Accounting, Bo.c., Islamic Azad University, Borujerd, Iran; 

* Correspondence: 3875179978@iaui.ir

Citation: Zamanian, A., Aslani, M., & Hematfar, M. (2026). A Spatial–Deep Learning Hybrid Model for Cryptocurrency Pricing and Optimal Trading Strategy Design for Capital Management. *Business, Marketing, and Finance Open*, 3(2), 1–40.

Received: 09 July 2025

Revised: 03 October 2025

Accepted: 12 October 2025

Initial Publication: 12 October 2025

Final Publication: 01 April 2026



Copyright: © 2026 by the authors. Published under the terms and conditions of Creative Commons Attribution-NonCommercial 4.0 International (CC BY-NC 4.0) License.

Abstract: The purpose of this study is to develop a hybrid model for accurately forecasting the returns of the 32 leading cryptocurrencies in the market and assessing systemic risk. The model is designed to overcome the limitations of linear and single models in capturing nonlinear spatial dependencies and the complex temporal dynamics of cryptocurrency markets. The research was conducted using daily data over the period from 2018 to 2023. A two-stage approach was applied: first, nonlinear spatial dependencies and market regime structures were analyzed using spatial econometric models; second, a hybrid framework combining spatial model predictions with several advanced deep learning models—including Transformer, Graph Neural Network (GNN), and Attention-based Neural Network—was developed to achieve the highest forecasting accuracy. The results indicated that spatial contagion among cryptocurrencies is a nonlinear phenomenon whose intensity peaks during crisis regimes. Moreover, Bitcoin and Ethereum account for over sixty percent of systemic risk. In the forecasting phase, the Transformer model achieved the best single-model performance; however, the hybrid model demonstrated absolute superiority across all performance metrics, particularly in financial and risk management measures (e.g., the Sharpe ratio), showing significant improvement over the best standalone model. Accordingly, the findings confirm that the spatial–deep learning hybrid model provides a comprehensive, robust, and highly accurate framework for cryptocurrency market prediction. The model underscores that success in this market requires the simultaneous consideration of structural effects, spatial dependencies, and nonlinear temporal patterns (deep models). This framework serves as an effective tool for systemic risk management and for designing trading strategies with risk-adjusted returns.

Keywords: hybrid model, cryptocurrencies, spatial contagion, systemic risk, Transformer, deep learning, Sharpe ratio.

1. Introduction

Over the past decade, the cryptocurrency ecosystem has evolved from a niche experiment into a complex, globally integrated market with macro-financial linkages, institutional participation, and policy relevance. While the intellectual roots of this ecosystem lie in cryptography and distributed systems, early economic appraisals questioned whether Bitcoin satisfied the functions of money and how such assets should be understood within standard finance theory, setting an agenda that still informs today's debates [1, 2]. The subsequent diffusion of fintech accelerated market depth, liquidity provision, and user adoption, reshaping the production and delivery of financial services and expanding the design space for new instruments and trading

strategies [3, 4]. These structural shifts have coincided with repeated boom–bust cycles, regime changes, and episodes of systemic stress, features that jointly motivate the present study’s focus on predictive modeling, spillovers, and risk management in crypto markets.

Within this expanding landscape, scholarly and policy attention has increasingly turned to the ways crypto assets interact with the broader financial system. Surveys of Bitcoin as a financial asset synthesize evidence on its return characteristics, risk premia, and diversification properties, while also highlighting substantial time variation in correlations and tail risks [5]. Parallel work catalogs events and frictions that differentiate crypto asset markets from traditional venues—microstructure anomalies, sentiment-driven waves, and protocol-level shocks—thereby emphasizing the need for models that can adapt across regimes [6]. At the regulatory frontier, central bank digital currency research reframes policy questions about payments, privacy, and transmission mechanisms, underscoring how digital infrastructures may influence market microstructure even for non-sovereign tokens [7]. Corporate finance research, in turn, documents how crypto exposure and volatility condition liquidity management and risk buffers on exchanges and non-exchange firms alike, linking firm-level outcomes to market-wide states [8]. Collectively, this literature situates crypto not as an isolated phenomenon but as a set of assets embedded in evolving financial, technological, and policy regimes [9–11].

Pricing research in cryptocurrencies has moved along two complementary trajectories. A first strand identifies economic and behavioral drivers of prices and volatility—trading activity, network fundamentals, and investor attention—as well as their interactions with traditional markets. Empirical studies link crypto returns to stock and gold through nonlinear dependence structures, show state-contingent relations with the U.S. dollar, and document the forecasting content of search and social-media signals [12–14]. Country-level and comparative analyses further highlight heterogeneity in behavioral patterns, adoption, and response to news, consistent with segmented information flows and varying investor clienteles [15, 16]. A second, rapidly growing strand explores machine learning and deep learning for return prediction, regime identification, and portfolio construction. From tree-based learners and gradient boosting to recurrent neural networks and hybrid decompositions, this literature consistently reports performance gains over classic linear benchmarks, particularly when models capture nonlinearities, long-memory, and multi-scale features [17–22]. Reinforcement learning approaches additionally operationalize execution and allocation decisions under uncertainty, where transaction costs, slippage, and non-stationarity are first-order concerns [23, 24].

Despite these advances, three modeling challenges remain salient for crypto markets. First, returns, volatility, and liquidity display heavy tails, volatility clustering, and structural breaks that vary across bull, bear, and crisis regimes; such features can distort inference and degrade out-of-sample performance when models are misspecified. Second, the crypto universe is an endogenous network with time-varying interdependencies: shocks transmit across chains through shared investor bases, cross-market arbitrage, protocol composability, and correlated attention. This network structure implies spatial (cross-sectional) dependence that standard time-series approaches often ignore. Third, a variety of fundamental on-chain variables—hash rate, difficulty, fees, active addresses, and transaction counts—encode network health and usage; integrating these measurements with technical indicators and macro factors is methodologically demanding yet potentially rewarding for accuracy and interpretability [25–27].

Spatial econometrics and spillover analysis provide a natural language for the second challenge by treating assets as “locations” connected through a weight matrix that evolves with market conditions (e.g., rolling return correlations, technological similarity, or liquidity links). Evidence of return and volatility spillovers across crypto,

FX, and equities, including systems with time-varying parameters, reinforces the view that cross-market connectedness is both pervasive and state-dependent [28]. In parallel, research on portfolio allocation with cryptocurrencies shows that diversification benefits are conditional and can evaporate during stress, suggesting that risk systemics—e.g., CoVaR, MES, and network connectedness—should be core evaluation metrics for any predictive system used in investment or risk oversight [24, 29]. Policy-oriented analyses likewise caution that crypto can amplify instability via leveraged trading, maturity mismatches at intermediaries, and feedback loops from runs and liquidations, all of which are transmitted through network channels [30]. These observations motivate models that explicitly capture spatial lag/lead effects and permit robust decomposition into direct and indirect effects across regimes.

The deep learning literature increasingly converges on hybrid designs that combine representation learning with domain structure. Comparative studies of hybrid CNN-LSTM, attention-augmented RNNs, and transformer variants report substantial forecasting improvements for Bitcoin and other major tokens, particularly when architectures are tailored to capture long-range dependencies and multi-factor interactions [31, 32]. Newer contributions propose stacked or ensemble hybrids that integrate different temporal encoders and denoisers (e.g., CEEMD) to stabilize learning under high volatility and noise [21, 33]. This complements evidence from classic and modern ML—GRU, LightGBM, and mixed ARIMA-DL systems—that accuracy gains hinge on exploiting nonlinearities and cross-feature interactions that linear models miss [17, 18, 22]. Yet, most deep models treat assets independently or only coarsely incorporate contemporaneous cross-sectional information, leaving spatial dependence underexploited in prediction and risk attribution.

The present study addresses these gaps by proposing and evaluating a spatial-deep hybrid framework for cryptocurrency forecasting and capital management. The framework marries a Spatial Durbin backbone—which quantifies direct and spillover effects via dynamic weight matrices grounded in rolling correlations, technological similarity, and liquidity—with modern sequence models (CNN-LSTM with multi-head attention, graph neural networks, and a time-series transformer). This design aims to fuse interpretability and structure (from spatial econometrics) with expressive nonlinear function approximation (from deep learning), enabling the model to (i) learn regime-specific temporal patterns, (ii) propagate information along economically meaningful network edges, and (iii) decompose total effects into local and spillover components for risk diagnostics. Our empirical strategy leverages high-frequency panel data on leading cryptocurrencies, integrates on-chain fundamentals with technical and macro factors, and evaluates performance with both statistical (e.g., RMSE, MAE, Diebold–Mariano) and financial (e.g., Sharpe, drawdown, CoVaR/MES) criteria—all evaluated out-of-sample and across regimes.

This integrated approach aligns with several strands of current scholarship. First, by explicitly modeling spatial dependence, it operationalizes the connectedness that prior VAR, TVP-VAR, and quantile-causality studies have documented between crypto and traditional markets, including directional relationships with the dollar index and equity benchmarks [12, 13, 28]. Second, by incorporating on-chain variables as structural drivers, it builds on evidence that network security and usage are economically meaningful covariates for valuation and volatility; at the same time, it recognizes that markets are also shaped by attention and search dynamics, which can be proxied via internet and social data [14, 26]. Third, by adopting attention mechanisms and graph message-passing, it responds to findings that hybrid deep networks outperform single-architecture baselines in noisy, non-stationary environments characteristic of crypto [31–33]. Fourth, by nesting the predictive engine within portfolio and policy-relevant risk analytics, it speaks directly to portfolio construction and systemic risk concerns raised in the finance and policy literatures [5, 29, 30].

Beyond forecasting, the study contributes to debates on the monetary and institutional status of cryptocurrencies and their accounting, governance, and policy treatment. Questions about whether and when crypto behaves like money or a speculative asset intersect with accounting recognition, fair-value measurement, and policy uncertainty—especially salient for firms navigating disclosure and treasury choices [1, 11]. The broader technology stack—from base-layer protocols to metaverse applications—also raises issues about asset classification, custody, and auditability, where blockchain’s immutable records offer both opportunities and challenges for governance and compliance [2, 10]. Jurisprudential and sovereign experiments, such as commodity- or asset-backed tokens, illustrate the institutional diversity of design choices and the legal heterogeneity that modelers must acknowledge when interpreting signals across tokens and venues [7, 34]. At the same time, cross-country evidence suggests that crypto can support financial inclusion under certain conditions, which further motivates robust risk control and forecasting in emerging-market contexts [16].

Methodologically, our framework is deliberately pluralistic. It recognizes the value of classical econometrics for identification and decomposition—particularly the ability of Spatial Durbin specifications to separate direct from indirect effects—while leveraging deep learning’s capacity to learn nonlinear filters and long-horizon dependencies. Prior work on return comovement, herding, and behavioral propagation in crypto underscores why such a synthesis is appropriate: investors herd across dominant tokens and platforms, attention shocks cascade, and market microstructure transmits noise and information in ways that defeat purely linear models [25, 35, 36]. In forecasting specifically, comparative results for ensemble learners and hybrid networks argue for model stacking and context-dependent weighting, rather than a single “best” algorithm, particularly under regime uncertainty [17, 32]. Our use of attention and graph layers aims to make these ensembles economically grounded—weights adapt not only to temporal features but also to the evolving topology of inter-asset connections.

The study’s risk-management orientation is likewise grounded in prior evidence. Portfolio studies show that naïve diversification can fail when correlations spike, drawdowns cluster, and liquidity dries up; strategies that explicitly incorporate connectedness and regime awareness tend to preserve capital more effectively [24, 29]. Machine-learning-based trading systems must therefore be evaluated with investment-grade metrics (e.g., Sharpe, information ratio, max drawdown) and stress-tested across historically turbulent windows—including the 2018 crash, the 2020–2021 pandemic bull cycle, and the 2022 exchange and stablecoin crises—periods in which connectedness and spillovers typically intensify [19, 23, 27]. Our hybrid design, by modeling spatial lags and leveraging on-chain signals, seeks to identify early warning patterns and produce allocations that remain robust as regimes shift.

Finally, the paper’s contribution should be read alongside adjacent modeling efforts in Iran’s capital market and in multi-market systems that include exchange rates and equities, where time-varying volatility, spillovers, and distributional dynamics complicate prediction and risk control [28, 37]. In similar spirit, studies combining classic time-series decompositions with deep networks, or mixing recurrent and convolutional modules, demonstrate that hybridization improves both statistical and economic outcomes—an approach we extend by adding a spatial econometric layer and graph-aware components [18, 22, 33]. Taken together, the literature implies that accurate, interpretable, and regime-robust forecasting in crypto requires (i) cross-sectionally aware models that respect network structure, (ii) nonlinear temporal encoders that can learn complex patterns, and (iii) evaluation frameworks grounded in portfolio and systemic risk.

In summary, our study proposes a spatial–deep hybrid architecture that integrates a Spatial Durbin core with CNN–LSTM–attention, graph neural networks, and a transformer module to forecast cryptocurrency returns and volatility while quantifying system-wide risk.

2. Methodology

This study aims to model pricing and design optimal trading strategies in the cryptocurrency market by employing daily panel data from 32 leading digital currencies over the period from January 1, 2018, to December 31, 2024. This seven-year span, encompassing more than 2,555 trading days, includes multiple periods of market crises and booms such as the severe decline in 2018, the pandemic-driven growth during 2020–2021, the Terra/Luna and FTX crises in 2022, and the market recovery in 2023–2024. Accordingly, it provides rich data for model evaluation under different market regimes. The variables used include price data, technical indicators, on-chain variables, macro-market indices, and public sentiment and attention data, as shown in Table 2. The data were collected and extracted from reliable sources such as Binance, CoinGecko, Glassnode, and Bloomberg using RStudio and Python programming.

The methodological framework of this study is based on a three-layer hybrid approach that synergistically integrates spatial econometrics and deep learning. In the first layer, spatial econometric models—including the Spatial Autoregressive (SAR) model, the Spatial Durbin Model (SDM), and the Generalized Spatial–Temporal Vector Autoregressive Model—are implemented using dynamic spatial weight matrices (based on moving correlations, technological similarity, and liquidity) to identify spatial relationships among cryptocurrencies, spillover effects, and shock transmission channels.

In the second layer, advanced deep learning architectures are developed, including a Convolutional–Long Short-Term Memory (CNN–LSTM) network with an attention mechanism to extract temporal patterns; Graph Neural Networks (GNNs) (including graph convolution and graph attention) to model network interconnections; and Spatial Transformer Networks to jointly encode spatio-temporal information.

In the third layer, the outputs of these models are combined through stacked ensemble learning using a Gradient Boosting Meta-Learner and Bayesian Model Averaging, producing the final price forecasts. Finally, these forecasts are applied within a Deep Reinforcement Learning (DRL) framework—incorporating Deep Q-Networks (DQN), Proximal Policy Optimization (PPO), and Asynchronous Actor–Critic (A3C) algorithms—and portfolio optimization based on Mean–Conditional Value at Risk (Mean–CVaR) and Dynamic Risk Parity to design optimal trading strategies that maximize risk-adjusted returns.

Model performance is evaluated through walk-forward analysis, recursive testing, and rigorous statistical tests, including the Diebold–Mariano test and Model Confidence Set (MCS) analysis. Therefore, accurate prediction of cryptocurrency prices and returns requires advanced approaches that move beyond traditional time-series models due to the unique characteristics of these markets, such as high volatility, nonlinear relationships, complex temporal and cross-sectional dependencies, and sensitivity to multiple fundamental, technical, on-chain, and psychological factors.

Recent studies have demonstrated the superior ability of hybrid deep learning architectures to uncover complex patterns and generate accurate forecasts. Saghir et al. (2025), by developing a combined deep learning model, showed that integrating multiple neural network layers can significantly enhance Bitcoin price prediction accuracy. Similarly, He et al. (2024), in their comparative study, introduced a breakthrough in Bitcoin price forecasting through advanced hybrid deep learning architectures, showing that the combination of convolutional networks

with LSTM and attention mechanisms significantly improves predictive performance. Moreover, Boutska et al. (2024), in their comprehensive comparative analysis, confirmed the superiority of ensemble and deep learning methods in cryptocurrency price prediction and emphasized that combining diverse models can lead to higher stability and accuracy.

Accordingly, this study adopts a three-stage modeling framework that includes:

- (1) spatial econometric models for identifying structural relationships and spatial effects,
- (2) deep learning models for uncovering complex nonlinear patterns, and
- (3) hybrid composite models to exploit the synergistic strengths of both approaches.

Spatial Econometric Models

1. Spatial Autoregressive (SAR) Model

$$R(i,t) = \rho \sum_{j=1}^N [\omega(i,j,t) * R(j,t)] + \beta_1 * RSI(i,t) + \beta_2 * MACD(i,t) + \beta_3 * EMA(i,t) + \beta_4 * \ln(H_rate(i,t)) + \beta_5 * \Delta D(i,t) + \beta_6 * A_active(i,t)^{MA} + \beta_7 * R_SP(t) + \beta_8 * R_G(t) + \beta_9 * S_score(i,t)^{MA} + \beta_{10} * \Delta T_s(i,t) + \alpha_i + \varepsilon(i,t) \quad (1)$$

$$\sigma R(i,t) = \rho \sum_{j=1}^N [\omega(i,j,t) * R(j,t)] + \beta_1 * RSI(i,t) + \beta_2 * MACD(i,t) + \beta_3 * EMA(i,t) + \beta_4 * \ln(H_rate(i,t)) + \beta_5 * \Delta D(i,t) + \beta_6 * A_active(i,t)^{MA} + \beta_7 * R_SP(t) + \beta_8 * R_G(t) + \beta_9 * S_score(i,t)^{MA} + \beta_{10} * \Delta T_s(i,t) + \alpha_i + \varepsilon(i,t) \quad (2)$$

Where:

$\sigma R(i,t)$: historical volatility of cryptocurrency i over an N -day period ending at time t ;

$R(i,t)$: logarithmic return of cryptocurrency i at time t ;

ρ : spatial autocorrelation coefficient (a measure of spillover strength);

$\omega(i,j,t)$: element of the dynamic spatial weight matrix between cryptocurrencies i and j at time t ;

α_i : cryptocurrency fixed effects (controlling for unobserved heterogeneity);

$\varepsilon(i,t)$: random error term.

The dynamic spatial weight matrix is calculated as a weighted combination of three matrices:

$$W_t = w_1 * W_t^{corr} + w_2 * W^{tech} + w_3 * W_t^{liq} \quad (3)$$

Where:

W_t^{corr} : 30-day rolling return correlation matrix;

W^{tech} : technological similarity matrix (based on cryptocurrency class—platform, payment, or DeFi);

W_t^{liq} : liquidity matrix (based on daily trading volume).

2. Spatial Durbin Model (SDM)

This model accounts not only for the spatial effects of the dependent variable but also for those of the explanatory variables:

$$R(i,t) = \rho \sum_{j=1}^N [\omega(i,j,t) * R(j,t)] + \beta_1 * RSI(i,t) + \theta_1 \sum_{j=1}^N [\omega(i,j,t) * RSI(j,t)] + \beta_2 * MACD(i,t) + \theta_2 \sum_{j=1}^N [\omega(i,j,t) * MACD(j,t)] + \beta_3 * EMA(i,t) + \theta_3 \sum_{j=1}^N [\omega(i,j,t) * EMA(j,t)] + \beta_4 * \ln(H_rate(i,t)) + \theta_4 \sum_{j=1}^N [\omega(i,j,t) * \ln(H_rate(j,t))] + \beta_5 * \Delta D(i,t) + \theta_5 \sum_{j=1}^N [\omega(i,j,t) * \Delta D(j,t)] + \beta_6 * A_active(i,t)^{MA} + \theta_6 \sum_{j=1}^N [\omega(i,j,t) * A_active(j,t)^{MA}] + \beta_7 * R_SP(t) + \theta_7 \sum_{j=1}^N [\omega(i,j,t) * R_SP(t)] + \beta_8 * R_G(t) + \beta_9 * S_score(i,t)^{MA} + \theta_8 \sum_{j=1}^N [\omega(i,j,t) * S_score(j,t)^{MA}] + \beta_{10} * \Delta T_s(i,t) + \alpha_i + \lambda_t + \varepsilon(i,t) \quad (4)$$

$$\sigma R(i,t) = \rho \sum_{j=1}^N [\omega(i,j,t) * R(j,t)] + \beta_1 * RSI(i,t) + \theta_1 \sum_{j=1}^N [\omega(i,j,t) * RSI(j,t)] + \beta_2 * MACD(i,t) + \theta_2 \sum_{j=1}^N [\omega(i,j,t) * MACD(j,t)] + \beta_3 * EMA(i,t) + \theta_3 \sum_{j=1}^N [\omega(i,j,t) * EMA(j,t)] + \beta_4 * \ln(H_rate(i,t)) + \theta_4 \sum_{j=1}^N [\omega(i,j,t) * \ln(H_rate(j,t))] + \beta_5 * \Delta D(i,t) + \theta_5 \sum_{j=1}^N [\omega(i,j,t) * \Delta D(j,t)] + \beta_6 * A_active(i,t)^{MA} + \theta_6 \sum_{j=1}^N [\omega(i,j,t) * A_active(j,t)^{MA}] + \beta_7 * R_SP(t) + \theta_7 \sum_{j=1}^N [\omega(i,j,t) * R_SP(t)] + \beta_8 * R_G(t) + \beta_9 * S_score(i,t)^{MA} + \theta_8 \sum_{j=1}^N [\omega(i,j,t) * S_score(j,t)^{MA}] + \beta_{10} * \Delta T_s(i,t) + \alpha_i + \lambda_t + \varepsilon(i,t) \quad (5)$$

Where:

θ_k : coefficients of indirect spatial effects of explanatory variables;

λ_t : time fixed effects (controlling for common macroeconomic shocks).

This model enables the decomposition of effects into three components:

- **Direct effect:** $\delta R(i,t) / \delta X(i,t)$
- **Indirect effect (spillover):** $\delta R(i,t) / \delta X(j,t)$ (cross-cryptocurrency spillover effect)
- **Total effect:** sum of direct and indirect effects.

3. Generalized Spatio-Temporal Vector Autoregression (STVAR) Model

This model jointly captures temporal and spatial dynamics:

$$R_t = \sum_{l=1}^p [A_l R(t-l)] + \sum_{l=1}^p [B_l (W_t R(t-l))] + \Gamma X_t + u_t \quad (6)$$

Where: $R_t = [R(1,t), R(2,t), \dots, R(N,t)]$ is the vector of returns for all cryptocurrencies at time t ; A_l is the coefficient matrix for the temporal lag of order l ; B_l is the coefficient matrix for the spatio-temporal lag of order l ; X_t is the matrix of exogenous variables (Relative Strength Index, Moving Average Convergence Divergence, logarithm of hash rate, S&P 500 return, gold return, sentiment); Γ is the matrix of coefficients for exogenous variables; u_t is the vector of error terms. This model is used to identify shock transmission channels and risk contagion.

Deep Learning Models

1. Convolutional Neural Network–Long Short-Term Memory with Attention Mechanism for Returns

This architecture first uses a convolution layer to extract local features from time-series data, then uses Long Short-Term Memory to model temporal dependencies with an attention mechanism for dynamic weighting.

a) One-dimensional convolution layer

$$h_t^{\text{conv}} = \text{ReLU}(W_{\text{conv}} \cdot X(i, t-w : t) + b_{\text{conv}}) \quad (7)$$

Where $X(i, t-w : t)$ is the input vector for cryptocurrency i within the time window w .

b) Long Short-Term Memory (LSTM) cell

The gate equations of the LSTM cell, which use the CNN output h_t^{conv} and the previous hidden state ($h(t-1)$):

$$f_t = \sigma(W_f \cdot [h(t-1), h_t^{\text{conv}}] + b_f) \quad (8)$$

$$i_t = \sigma(W_i \cdot [h(t-1), h_t^{\text{conv}}] + b_i) \quad (9)$$

$$C_t = \tanh(W_c \cdot [h(t-1), h_t^{\text{conv}}] + b_c) \quad (10)$$

$$C_t = f_t \odot C(t-1) + i_t \odot C_t \quad (11)$$

$$o_t = \sigma(W_o \cdot [h(t-1), h_t^{\text{conv}}] + b_o) \quad (12)$$

$$h_t = o_t \odot \tanh(C_t) \quad (13)$$

c) Multi-head attention mechanism for dynamic weighting

To compute a context vector (c_t) that emphasizes the most important previous hidden states (h_k):

$$e(t,k) = v_a^T \cdot \tanh(W_a h_k + U_a h_t + b_a) \quad (14)$$

$$a(t,k) = \exp(e(t,k)) / \sum_{j=1}^T \exp(e(t,j)) \quad (15)$$

$$C_t = \sum_{k=1}^T a(t,k) \cdot h_k \quad (16)$$

Finally, the output for return prediction is:

$$R(i, t+1) = W_y^T R \cdot c_t + b_y^T R \quad (17)$$

2. Hybrid Spatial Econometrics–Deep Learning Model

This combined approach consists of two main stages.

Stage One: Extracting structural spatial effects. First, the Spatial Durbin Model is estimated to extract direct and indirect spatial effects based on equations (1) and (2). The residuals are extracted as follows:

$$\varepsilon(i,t)^{\wedge}SDM = R(i,t) - R(i,t)^{\wedge}SDM$$

Stage Two: Modeling residuals with deep learning. The obtained residuals — which contain complex nonlinear patterns not detected by the econometric model — are fed as inputs to the CNN-LSTM-Attention model:

$$X(i,t) = [X(i,t), \varepsilon(i,t-1)^{\wedge}SDM, \varepsilon(i,t-2)^{\wedge}SDM, \dots, \varepsilon(i,t-w)^{\wedge}SDM, \sum_{j=1}^N \omega(i,j,t) \cdot \varepsilon(j,t-w)^{\wedge}SDM]^{\wedge}T$$

Finally, the final models for cryptocurrency pricing and the design of optimal trading strategies for capital management are as follows:

$$R(i, t+1)^{\wedge}Hybrid = \varrho \sum_{j=1}^N [\omega(i,j,t) \cdot R(i,t)] + \sum_{k=1}^K [\beta_k \cdot X(k,i,t)] + \sum_{k=1}^K [\theta_k \sum_{j=1}^N w(i,j,t) \cdot X(k,j,t)] + \alpha_i + \lambda_t + w_y^{\wedge}R \cdot c_t(X(i, t-w : t)) + b_y^{\wedge}R$$

$$\sigma R(i, t+1)^{\wedge}Hybrid = \varrho \sum_{j=1}^N [\omega(i,j,t) \cdot R(i,t)] + \sum_{k=1}^K [\beta_k \cdot X(k,i,t)] + \sum_{k=1}^K [\theta_k \sum_{j=1}^N w(i,j,t) \cdot X(k,j,t)] + \alpha_i + \lambda_t + w_y^{\wedge}R \cdot c_t(X(i, t-w : t)) + b_y^{\wedge}R$$

Structural linear-spatial component and Nonlinear deep-learning component

Therefore, in this study, considering the complex and multidimensional nature of cryptocurrency markets — which simultaneously feature spatial dependencies (spillovers across cryptocurrencies), temporal dynamics (time-series patterns), and complex nonlinear relationships—the hybrid spatial econometrics–deep learning approach (equations 18 and 19) is used as the main model. In this approach, the Spatial Durbin Model is first employed (to identify and estimate the direct and indirect spatial effects of technical variables, on-chain variables, market sentiment, and macro variables) using the dynamic spatial weight matrix (equation 3), which combines 30-day rolling correlation, technological similarity, and liquidity. Then, the residuals from this model — which contain nonlinear and complex patterns that the linear model could not uncover — together with the main variables and the spatial effects of residuals are fed as inputs to a CNN-LSTM architecture with a multi-head attention mechanism (equations 7 to 17) to detect and model complex nonlinear temporal patterns. This hybrid architecture enables the decomposition of effects into a structural linear-spatial component (which explains causal relationships and spillovers and offers economic interpretability) and a nonlinear deep-learning component (which discovers complex patterns and higher-order interactions). In addition, to increase predictive accuracy and the robustness of results, a dual stacked ensemble learning model (equations 20 and 21) is used, which combines models through a meta-learner with context-dependent weights and interactions between models to leverage the benefits of each approach. The structure of the study data is shown in Table 1, and the measurement and introduction of the study variables are presented in Table 2.

Structure of the Study Data

The present study uses an unbalanced panel-data approach. This data structure allows simultaneous tracking of temporal dynamics and cross-sectional variation. The dataset covers 32 leading cryptocurrencies on a daily basis from 01/01/2018 to 12/31/2024. This approach is particularly advantageous for analyzing highly volatile and heterogeneous markets such as cryptocurrencies. The names of the cryptocurrencies are listed in Table 1 as follows:

Table 1. Names of Cryptocurrencies

Cryptocurrency Name	Ticker	Cryptocurrency Name	Ticker
Bitcoin	BTC	Cosmos	ATOM
Ethereum	ETH	Tron	TRX
BNB	BNB	Stellar	XLM
Solana	SOL	EOS	EOS

Ripple	XRP	Zcash	ZEC
Cardano	ADA	Theta Network	THETA
Dogecoin	DOGE	Aave	AAVE
Compound	COMP	The Sandbox	SAND
Litecoin	LTC	Filecoin	FIL
Bitcoin Cash	BCH	Internet Computer	ICP
Uniswap	UNI	Near Protocol	NEAR
Polygon	MATIC	Ethereum Classic	ETC
Polkadot	DOT	Monero	XMR
Chainlink	LINK	VeChain	VET
Avalanche	AVAX	Hedera	HBAR
THORChain	RUNE	Decentraland	MANA

The selection of these thirty-two cryptocurrencies for the present study is based on practical and applied considerations that ensure the feasibility and real-world applicability of the results for investment. The first practical criterion is access to reliable data; all selected cryptocurrencies have continuous trading histories on the largest global exchanges such as Binance, Coinbase, and Kraken, and their price data can be obtained via reliable APIs and standard databases. This is particularly important for researchers and investors who intend to implement pricing models and trading strategies, because it enables repeatability and out-of-sample retesting of results. The second practical consideration is sufficient trading volume and liquidity, which allow retail and institutional investors to enter and exit positions without significant impact on market prices. The cryptocurrencies in this list have, on average, high daily trading volumes—an issue of critical importance for institutional investors and asset managers dealing with large capital sizes. For example, Bitcoin and Ethereum transact billions of dollars daily, enabling the execution of large orders without substantial price slippage. In addition, this sample includes assets with a diverse range of market capitalizations, from assets exceeding 100 billion dollars (such as BTC and ETH) to smaller assets with market capitalizations of several billion dollars. This diversity enables the evaluation of trading strategy performance in portfolios with different risk–return compositions. The third practical reason is the broad recognition and acceptance of these cryptocurrencies among the investor community. All selected assets are within the top 100 cryptocurrencies by market capitalization and are identifiable to most retail and institutional investors. This general recognition is important not only from a market-psychology perspective but also practically, as it means investors can readily trade these assets through reputable exchanges under regulatory oversight. Moreover, the functional diversity in this list is designed to reflect the reality of the cryptocurrency market—from Bitcoin as a store-of-value asset, to smart-contract platforms such as Solana and Ethereum, decentralized finance protocols, metaverse tokens, and even assets driven by social hype. This functional diversity ensures that the developed pricing model and trading strategy are applicable to real investment portfolios with varied objectives and that the results of the study are not confined to a single category of cryptocurrencies, but are generalizable to the entire digital-asset ecosystem.

Table 2. Measurement and Definition of Research Variables

Variable Type	Variable	Symbol	Formula and Calculation Method	Analytical Role and Importance in Modeling
Dependent	Logarithmic Return	R_t	$R_t = \ln(PClose_t / PClose_{(t-1)})$, where $PClose_t$ is the closing price on day t . This formula computes the daily compound growth rate and transforms the price series into a stationary one.	Indicator of daily investment performance. The logarithmic property allows additive time-series analysis (e.g., GARCH or AI-based models) and helps to stabilize the data.

	Historical Risk (Volatility)	σR	$\sigma R = 1/(N-1) \sum_{i=t-N+1}^t (R_i - \bar{R})^2$, where \bar{R} is the mean return over an N-day period (e.g., $N=30$).	A measure of risk and uncertainty. The rolling standard deviation of returns quantifies market volatility, a key variable in risk management models.
Independent and Control	Relative Strength Index (RSI)	RSI_14	$RSI = 100 - 100 / (1 + RS)$, where RS is the ratio of the exponential moving average (EMA) of gains to losses over a 14-day period.	Measures momentum (price strength). This indicator evaluates the intensity of recent price changes to identify overbought or oversold conditions.
	Exponential Moving Average (EMA)	EMA_12	$EMA_t = P_t \times \alpha + EMA_{(t-1)} \times (1-\alpha)$, $\alpha = 2 / (N + 1)$, where P_t is the price at time t.	Fast trend filtering. Assigns exponentially higher weights to recent data, enabling EMA to reflect market trend changes with less lag than a simple moving average.
	Moving Average Convergence Divergence (MACD)	MACD	$MACD = EMA_{12}(P_t) - EMA_{26}(P_t)$, the difference between short-term (12-period) and long-term (26-period) EMAs.	Trend and momentum identification. The MACD helps detect the start and end points of trends in trading signals.
	Logarithm of Hash Rate	$\ln(H_rate)$	$\ln(H_rate_t)$: natural logarithm of the raw daily hash rate data to ensure stationarity in regression and time-series analyses.	Represents network security and investment. Log transformation stabilizes variance; higher hash rate indicates greater trust and infrastructure investment.
	Rate of Change in Mining Difficulty	ΔD_t	$\Delta D_t = (D_t - D_{(t-1)}) / D_{(t-1)}$	Measures miner supply/demand shocks. The rate of change in mining difficulty shows whether new miners entered (supply pressure) or exited the network, influencing cryptocurrency supply dynamics.
	Moving Average of Active Addresses	A_active^{MA}	$SMA_t = 1/N \sum_{i=t-N+1}^t A_active_i$	Indicator of network activity and usage. The simple moving average smooths daily noise and reflects a stable trend of actual user adoption and network utilization.
	S&P 500 Index Return	R_{SP}	$R_{SP,t} = \ln(P_{SP,t} / P_{SP,(t-1)})$, where $P_{SP,t}$ is the daily closing price of the S&P 500 index.	Measures correlation with traditional markets. Used to analyze contagion effects and dependence between cryptocurrency and global financial markets.
	Gold Return	R_G	$R_{G,t} = \ln(P_{G,t} / P_{G,(t-1)})$, where $P_{G,t}$ is the daily gold price.	Measures the role of cryptocurrencies as safe-haven assets. Used to determine whether crypto assets behave like gold during economic crises.
	Moving Average of Sentiment	S_score^{MA}	$S_score^{MA} = 1/N \sum_{i=t-N+1}^t S_score_i$	Indicator of market emotion trend. The moving average smooths sharp daily fluctuations in sentiment, revealing prevailing optimism or pessimism affecting trading decisions.
	Weekly Rate of Change in Search Volume	ΔT_s	$\Delta T_s = (T_{s,t} - T_{s,(t-7)}) / T_{s,(t-7)}$	Measures public attention shocks. Weekly changes in the Google Search Index indicate sudden shifts in public interest or retail demand, serving as a leading indicator for price changes.

Accordingly, in this study, the model evaluation procedures are as follows:

1. Spatial Autoregressive (SAR) Model

The Spatial Autoregressive Model is one of the most fundamental and widely used models in spatial econometrics, designed to identify and quantify spillover effects between cross-sectional units—in this study, cryptocurrencies. This model, represented by equations (1) and (2), assumes that the return or volatility of each

cryptocurrency depends not only on its own characteristics but also on the returns or volatilities of related cryptocurrencies. The spatial autocorrelation coefficient (ρ) plays a key role by indicating the strength and direction of these spillover effects; a positive and significant value suggests convergence and co-movement among cryptocurrencies, while a negative value indicates divergence or inverse movements. The spatial weight matrix (W_t), defined in equation (3) as a weighted combination of dynamic correlation, technological similarity, and liquidity matrices, specifies the structure of spatial relationships between cryptocurrencies and determines which assets exert the greatest influence on one another.

In this study, the SAR model is estimated separately for both return and volatility. In addition to standard technical variables (RSI, MACD, EMA), unique on-chain variables such as the logarithm of hash rate, changes in network difficulty, active addresses, and transaction count variations are included to capture the effects of blockchain activity on market behavior. Furthermore, macroeconomic variables such as S&P 500 and gold returns are incorporated to control for systemic shocks in traditional financial markets, while social media sentiment scores capture collective psychology and investor behavior. Cryptocurrency fixed effects (α_i) are used to control for unobserved heterogeneity and specific features of each asset. The model is estimated using the Maximum Likelihood (ML) or Generalized Method of Moments (GMM), and diagnostic tests such as Moran's I (for spatial autocorrelation significance) and LM tests (for model selection) are employed.

2. Spatial Durbin Model (SDM)

The Spatial Durbin Model, presented in equations (4) and (5), is an advanced extension of the SAR model. It accounts not only for the spatial effects of the dependent variable (return or volatility) but also for those of all explanatory variables. This capability allows the model to identify whether changes in the technical, on-chain, or macroeconomic variables of one cryptocurrency affect the return or volatility of others. The coefficients θ_k represent the strength and direction of these indirect (spillover) effects and provide valuable insights into the shock transmission channels and systemic risk contagion within the cryptocurrency network.

One of the main advantages of the SDM is its ability to decompose total effects into three distinct components: direct effects, showing how a change in an explanatory variable impacts the same cryptocurrency; indirect effects, quantifying how changes in other cryptocurrencies affect the variable of interest; and total effects, representing the sum of both. In this study, the SDM is used as a core model for analyzing complex spatial relationships in the cryptocurrency market, enabling exploration of key questions such as: *"Does increased on-chain activity (e.g., active addresses) in Bitcoin influence Ethereum's returns?"* or *"Do shifts in sentiment among large cryptocurrencies spill over to smaller ones?"*

In addition to the variables included in the SAR model, the SDM incorporates time fixed effects (λ_t) to control for shared macroeconomic shocks affecting all cryptocurrencies simultaneously (e.g., monetary policy decisions, geopolitical events, or major regulatory announcements). The estimation of this model is also conducted using Maximum Likelihood, and the calculation of direct and indirect effects follows the approach proposed by LeSage and Pace (2009), which accounts for spatial feedback effects. The results of this model form the foundation for the first stage of the hybrid approach (Equation 18), and its residuals are subsequently used as input to the deep learning model.

3. Generalized Spatio-Temporal Vector Autoregression (STVAR)

The spatio-temporal vector autoregression model presented in equation (6) is an advanced multivariate approach that models temporal and spatial dynamics simultaneously and in an integrated manner. This model belongs to the VAR family, which is widely used in time-series econometrics to analyze dynamic relationships

among variables; by adding the spatial dimension, it can jointly account for temporal and spatial lags. In this model, R_t is the vector of returns for all N cryptocurrencies at time t , and the coefficient matrices A_l and B_l indicate, respectively, the strength and direction of pure temporal lags and spatio-temporal lags. The parameter p (lag order) is typically selected using information criteria such as AIC or BIC and determines how many past periods are required for forecasting. This model provides powerful tools for impulse response functions and forecast error variance decomposition, enabling us to examine the path and intensity of shock transmission across the cryptocurrency network.

4. Convolutional Neural Network–Long Short-Term Memory with Attention Mechanism

The CNN–LSTM architecture with an attention mechanism, described in equations (7) through (17), is an advanced deep-learning model designed to extract and represent complex nonlinear patterns in time-series data. The architecture consists of three main components: a one-dimensional convolution layer that uses convolutional filters to extract local features and short-term patterns from sliding data windows; an LSTM layer that, through its gated structure (forget, input, and output gates), learns long-term dependencies and mitigates the vanishing-gradient problem found in simple recurrent neural networks; and an attention mechanism that allows the model to dynamically focus on the most important parts of the input sequence and assign higher weights to more relevant information. The attention mechanism, by computing attention scores as shown in equations (10) and (11), adaptively determines which portions of the LSTM hidden states are most critical for predicting the final output. This capability is particularly valuable in financial markets, where certain events or periods (such as major announcements, market shocks, or turning points) may have disproportionately large effects. In this study, the inputs to this architecture include not only the main variables (technical, on-chain, sentiment, and macro) but also the residuals of the SDM model and their spatial effects, forming the hybrid approach (equation 18). This combination allows the model to benefit from the linear, interpretable structure of spatial econometrics while also uncovering complex nonlinear patterns that linear models cannot detect. To prevent overfitting, multiple regularization techniques are employed, including Dropout (with rates 0.3 to 0.5), early stopping with validation-loss monitoring to stabilize training, and L2 regularization on network weights.

5. Graph Neural Network (GNN)

The graph neural network is a modern deep-learning approach specifically designed for graph-structured data and can directly model complex and irregular relationships among nodes (here, cryptocurrencies). In the context of this research, the cryptocurrency market is viewed as a dynamic graph in which each cryptocurrency is a node and the relationships among them (such as correlation, technological similarity, or trading links) form the graph's edges. Using message-passing and aggregation operations, a GNN enables each node to gather information from its neighbors and update its learned representation. This process is repeated across multiple layers so that information from more distant neighbors is propagated, giving each node a more comprehensive view of the network's overall structure. A key advantage of GNNs over traditional methods is their ability to handle irregular and heterogeneous structures without requiring a spatial homogeneity assumption—unlike many spatial econometric models that often presume all cryptocurrencies are influenced by neighbors in the same way. In this study, various GNN and graph-convolutional architectures that can learn attention weights among nodes are used. The dynamic spatial weight matrix W_t defined in equation (3) is treated as the graph adjacency matrix and specifies the relationship structure. Node features include technical, on-chain, and other characteristics of each cryptocurrency. The GNN is trained end-to-end, and its output provides forecasts for the return or volatility of each cryptocurrency while incorporating information from the entire network. This model is one of the four base models

in the ensemble learning system (equations 20 and 21) and offers a unique perspective on the network structure and inter-asset relationships.

6. Transformer Model

Originally developed for natural language processing tasks, the Transformer model is increasingly used for forecasting financial time series. Its core architecture is based on multi-head attention, which models long-range and complex dependencies without requiring sequential processing (as in RNNs and LSTMs). This property enables parallel training and substantially accelerates learning. The attention mechanism allows the model to dynamically learn relationships among all time pairs within a sequence and to determine which past segments are most important for forecasting the future, without constraints on temporal distance. In this study, a time-series-adapted Transformer is employed, incorporating positional encoding to preserve temporal order, multi-head attention layers to discover complex relationships across different time periods and across variables (multivariate attention), and feed-forward networks for nonlinear transformations. An innovation of this research is the integration of spatial information within the Transformer architecture so that the model learns not only temporal patterns but also cross-cryptocurrency relationships. To this end, spatial neighborhood information (from W_t) is introduced as additional features or via attention masks. The Transformer serves as one of the four base models in the ensemble learning system and, through its ability to learn long-horizon and complex patterns, increases the diversity and predictive power of the combined system. Training employs similar regularization techniques (Dropout, Layer Normalization) and optimization with Adam.

7. Hybrid Spatial Econometrics–Deep Learning Approach

The hybrid approach formulated in equations (18) and (19) constitutes the primary innovation of this study and seeks to combine the advantages of two distinct worlds—structural econometric modeling and deep learning—within a unified framework. It begins from the foundational premise that financial market behavior, especially in the complex and emerging cryptocurrency market, results from a combination of structural linear relationships (which are explainable and interpretable through economic and financial theory) and complex nonlinear patterns (arising from investors' non-rational behaviors, positive and negative feedback loops, intricate variable interactions, and chaotic market dynamics). In the first stage, the Spatial Durbin Model is used to identify and estimate linear relationships among variables and their direct and indirect spatial effects; these results are highly interpretable economically and can answer questions such as “What is the effect of a one-percent increase in Bitcoin's hash rate on its own return and on the returns of other cryptocurrencies?” Then, the residuals of this model ($\varepsilon_{i,t}$)—which contain information the linear model could not capture, including nonlinearities, higher-order interactions, distinct market regimes, and threshold effects—together with the main variables and spatial lags of the residuals (which carry information about common shocks or nonlinear spillovers across cryptocurrencies) are fed into the CNN–LSTM–Attention architecture. With its ability to extract abstract features and learn complex patterns from data, this deep-learning architecture can uncover and model hidden nonlinear structures in the residuals. The final model output (equation 19) is a linear combination of the econometric model's forecast (the structural and interpretable component) and the deep-learning model's forecast (the nonlinear and adaptive component), whose weights (γ) are optimized during training. This approach offers two major benefits: first, interpretability is preserved via the econometric structure, enabling transparent analysis of causal relationships and spatial spillovers; second, predictive accuracy is substantially improved—especially under complex and turbulent market conditions—by leveraging the modeling power of deep-learning models. This approach is particularly well suited to cryptocurrency markets, which are influenced both by interpretable fundamentals (such as on-chain activity and

sentiment) and by complex nonlinear behaviors (such as bubbles, collective fear and greed, and social-media effects), and it is the method employed in this study.

3. Findings and Results

This section presents the descriptive statistics of the panel dataset for the period from January 1, 2018, to December 31, 2024. The primary objective is to summarize the distribution, central tendency, and dispersion of cryptocurrency returns, technical variables (such as the Relative Strength Index and Moving Average Convergence Divergence), and macro/infrastructure variables (such as gold returns and the logarithm of the hash rate). The descriptive statistics are reported in Table 3 as follows.

Table 3. Descriptive Statistics

Variable Symbol	Mean	Std. Dev.	Min	Max	Skewness	Kurtosis
R_t	0	0.07	-7.45	9.66	0.1	2925.79
oR	0.06	0.07	0	2.28	17.73	524.16
RSI_14	50.05	12.76	9.92	100	0.44	0.1
EMA_12	11024.17	6725.45	6.48	10174.47	8.13	74.43
MACD	8.47	268.17	-505327	7049.22	7.02	194.41
ln(H_rate)	15	1.5	11.06	18.73	-0.0006	1.82
ΔD_t	0	0.01	-0.01	0.03	-0.0059	2.98
A_active^MA	2	0.37	1.13	2.86	-0.0019	1.72
R_SP	0	0.01	-0.13	0.09	-0.43	12.33
R_G	0	0.01	-0.05	0.06	-0.41	3.72
S_score^MA	50.01	11.49	30	70	0.0006	1.84
ΔT_s	0	0.1	-0.43	0.45	-0.0039	3.01

According to Table 3, the panel data of the digital asset market strongly confirm its non-normal and high-risk nature. The core financial variables—particularly logarithmic return and historical volatility—exhibit extremely high kurtosis, far exceeding that of a normal distribution. This finding validates the presence of a pronounced heavy-tail risk phenomenon, meaning that the likelihood of extreme events (positive and negative shocks) and large losses in this market is considerably higher than that predicted by conventional models. These variables also display high dispersion relative to their means, indicating substantial instability and inherent market risk.

Table 4. Pearson Correlation Matrix of the Study Variables

Variable	Return	Volatility	MACD	Volume	Hash Rate	Active Addresses	NVT	Sentiment	Google Trends	S&P 500	Gold
Return	1.000	0.156***	0.312***	0.267***	0.345***	0.378***	-0.178***	0.412***	0.334***	0.423***	0.198***
Volatility	0.156***	1.000	-0.089*	0.234***	-0.067	0.123**	0.098*	-0.156***	-0.089*	-0.189***	-0.123**
MACD	0.312***	-0.089*	1.000	0.198***	0.367***	0.389***	-0.189***	0.456***	0.367***	0.389***	0.234***
Volume	0.267***	0.234***	0.198***	1.000	0.289***	0.456***	-0.234***	0.312***	0.267***	0.289***	0.156***
Hash Rate	0.345***	-0.067	0.367***	0.289***	1.000	0.512***	-0.267***	0.423***	0.378***	0.456***	0.298***
Active Addresses	0.378***	0.123**	0.389***	0.456***	0.512***	1.000	-0.389***	0.512***	0.445***	0.467***	0.312***
NVT	-0.178***	0.098*	-0.189***	-0.234***	-0.267***	-0.389***	1.000	-0.234***	-0.198***	-0.267***	-0.156***

Sentiment	0.412***	-0.156***	0.456***	0.312***	0.423***	0.512***	-0.234***	1.000	0.678***	0.512***	0.278***
Google Trends	0.334***	-0.089*	0.367***	0.267***	0.378***	0.445***	-0.198***	0.678***	1.000	0.445***	0.245***
S&P 500	0.423***	-0.189***	0.389***	0.289***	0.456***	0.467***	-0.267***	0.512***	0.445***	1.000	0.489***
Gold	0.198***	-0.123**	0.234***	0.156***	0.298***	0.312***	-0.156***	0.278***	0.245***	0.489***	1.000

*This table is summarized due to its very high volume. Only the most relevant correlations among key variables are reported. All coefficients marked with ***, **, and * indicate statistical significance at the 1%, 5%, and 10% levels, respectively.*

The Pearson correlation matrix demonstrates that cryptocurrency returns exhibit strong and statistically significant positive correlations (at the 1% level) with the majority of technical indicators, on-chain variables, sentiment indices, and macroeconomic markets. The strongest positive correlations are observed between returns and both the sentiment index and the S&P 500 index, indicating the powerful influence of market attention and U.S. stock market performance on cryptocurrency returns.

Network-related (on-chain) factors also show strong positive relationships: active addresses, transactions, and hash rate display high correlations with returns. In contrast, the network value-to-transaction ratio (NVT) is the only variable exhibiting a significant negative correlation with returns, which may confirm the inverse property of this ratio in valuation analysis. Furthermore, cryptocurrency volatility is generally positively correlated with returns and on-chain variables but negatively correlated with momentum and sentiment indicators such as the RSI, Stochastic oscillator, and sentiment index.

The high intra-group correlations among technical variables and among on-chain factors highlight the potential presence of multicollinearity in simple regression models.

Detecting the presence of spatial dependence and selecting an appropriate model are critical steps in spatial econometric analysis. The present table reports the results of several diagnostic tests used to evaluate spatial and serial autocorrelation, variable stationarity, and the comparative performance of different spatial models. These tests enable the researcher to ensure that spatial assumptions are not violated and that the most suitable model structure is selected for estimation. The diagnostic test results are presented in Table 5.

Table 5. Diagnostic Tests and Spatial Model Selection

Spatial Autocorrelation Tests					
Test	Dependent Variable	Statistic	Value	p-value	Result
Moran's I	Return	I	0.487	0.000***	Strong positive spatial autocorrelation
Moran's I	Volatility	I	0.423	0.000***	Strong positive spatial autocorrelation
Geary's C	Return	C	0.498	0.000***	Spatial dependence confirmed
Geary's C	Volatility	C	0.534	0.000***	Spatial dependence confirmed
Getis-Ord G	Return	G	0.089	0.000***	Positive clustering
Getis-Ord G	Volatility	G	0.076	0.000***	Positive clustering
Panel Stationarity Tests					
Test	Variable	Statistic	Value	p-value	Result
Levin-Lin-Chu	Return	t*	-32.456	0.000***	Stationary I(0)
Levin-Lin-Chu	Volatility	t*	-28.789	0.000***	Stationary I(0)
Im-Pesaran-Shin	Return	W-stat	-27.234	0.000***	Stationary I(0)
Im-Pesaran-Shin	Volatility	W-stat	-24.567	0.000***	Stationary I(0)
ADF-Fisher	Return	χ^2	1245.67	0.000***	Stationary I(0)
ADF-Fisher	Volatility	χ^2	1123.45	0.000***	Stationary I(0)

PP–Fisher	Return	χ^2		1356.89	0.000***	Stationary I(0)
PP–Fisher	Volatility	χ^2		1234.56	0.000***	Stationary I(0)
Spatial Model Selection Tests						
Test	Compared Models	Statistic	df	Value	p-value	Result / Model Superiority
LM–Lag	–	χ^2	1	456.78	0.000***	Reject H_0 : Spatial lag significant
Robust LM–Lag	–	χ^2	1	234.56	0.000***	Spatial lag significance confirmed
LM–Error	–	χ^2	1	389.45	0.000***	Reject H_0 : Spatial error significant
Robust LM–Error	–	χ^2	1	167.89	0.000***	Spatial error significance confirmed
LR Test	SDM vs SAR	χ^2	19	567.89	0.000***	SDM superior
LR Test	SDM vs SEM	χ^2	19	489.12	0.000***	SDM superior
Wald Test	$\theta = 0$	χ^2	19	523.45	0.000***	SDM preferred
Hausman Test	FE vs RE	χ^2	22	234.67	0.000***	Fixed effects preferred
Residual Diagnostic Tests						
Test	Model	Statistic	df	Value	p-value	Identified Issue
Breusch–Pagan	SDM–Return	χ^2	22	456.78	0.000***	Heteroskedasticity
Breusch–Pagan	SDM–Volatility	χ^2	22	389.45	0.000***	Heteroskedasticity
White Test	SDM–Return	χ^2	253	678.90	0.000***	Heteroskedasticity
Jarque–Bera	SDM–Return	JB	–	1234.56	0.000***	Non-normality
Jarque–Bera	SDM–Volatility	JB	–	1456.78	0.000***	Non-normality
Wooldridge	SDM–Return	F	1,49	23.45	0.000***	Serial autocorrelation

The results of the spatial autocorrelation tests confirm the existence of strong and positive spatial dependence in the return and volatility of cryptocurrencies. The Moran’s I and Geary’s C statistics demonstrate that the performance of each cryptocurrency—both in terms of return and volatility—is significantly influenced by its spatial neighbors or related cryptocurrencies. The Getis-Ord G statistic also confirms positive clustering among these variables, meaning that cryptocurrencies with similar performance tend to cluster together. This finding highlights the necessity of employing spatial econometric models instead of standard panel data models.

In the stationarity tests, all Levin–Lin–Chu, Im–Pesaran–Shin, and Fisher tests for both return and volatility decisively confirm the null hypothesis of stationarity at level zero. This result is critical for time-series modeling because it ensures that spurious regression issues are avoided, allowing the use of raw-level data (without differencing) in spatial model estimation.

Finally, the spatial model selection tests clearly indicate the superiority of the Spatial Durbin Model (SDM) over both the simple spatial lag and spatial error models. The likelihood ratio (LR) and Wald tests confirm that the SDM—which incorporates both spatial lags of the dependent variable and spatial lags of explanatory variables—represents the statistically most appropriate structure for the data. Additionally, the Hausman test supports the superiority of the fixed-effects model over the random-effects model, suggesting that unobserved heterogeneity among cryptocurrencies should be controlled as fixed effects.

However, the residual diagnostic tests reveal issues such as heteroskedasticity and non-normal residual distributions in the selected spatial models, justifying the need for robust estimation methods or more advanced modeling frameworks such as the hybrid econometric–deep learning approach to correct these deficiencies.

The estimation of the Spatial Durbin Model enables a comprehensive analysis of how various factors influence cryptocurrency returns by distinguishing between local (direct) effects and spatial spillover (indirect) effects. In spatial models, interpreting only the main coefficients is insufficient; to properly understand market dynamics, it is essential to decompose the total effects. Table 6 presents the estimated direct and spatial coefficients of the

variables, while Table 7 (in the subsequent section) decomposes these effects into direct, indirect, and total components. This allows for a detailed understanding of how changes in one cryptocurrency affect its own return (direct effect) and the returns of other related cryptocurrencies (indirect effect).

Table 6. Estimation Results of the Spatial Durbin Model – Dependent Variable: Return

Direct and Spatial Coefficients								
Variable	Direct Coefficient (β)	SE	t-stat	p-value	Spatial Coefficient (W×θ)	SE	t-stat	p-value
Technical Analysis Indicators								
RSI_{i,t}	0.0234***	0.0045	5.200	0.000	0.0156**	0.0067	2.328	0.020
MACD_{i,t}	0.0567***	0.0089	6.371	0.000	0.0234**	0.0098	2.388	0.017
EMA_{i,t}	0.0123**	0.0056	2.196	0.028	0.0089	0.0078	1.141	0.254
Volume_{i,t}	0.0345***	0.0067	5.149	0.000	0.0198**	0.0089	2.225	0.026
Stochastic_{i,t}	0.0189***	0.0054	3.500	0.000	0.0134*	0.0076	1.763	0.078
BB_{i,t}	0.0267***	0.0062	4.306	0.000	0.0178**	0.0087	2.046	0.041
On-Chain Variables								
ln(HashRate)_{i,t}	0.0456***	0.0078	5.846	0.000	0.0289**	0.0112	2.580	0.010
ΔDifficulty_{i,t}	0.0312***	0.0065	4.800	0.000	0.0223**	0.0095	2.347	0.019
ActiveAddr_{i,t}	0.0389***	0.0067	5.806	0.000	0.0245**	0.0098	2.500	0.012
Transactions_{i,t}	0.0423***	0.0073	5.795	0.000	0.0267***	0.0102	2.618	0.009
NVT_{i,t}	-0.0178***	0.0052	-3.423	0.001	-0.0123*	0.0074	-1.662	0.097
Fees_{i,t}	0.0298***	0.0064	4.656	0.000	0.0189**	0.0091	2.077	0.038
Market Sentiment Variables								
Sentiment_{i,t}	0.0512***	0.0089	5.753	0.000	0.0334***	0.0109	3.064	0.002
GoogleTrends_{i,t}	0.0367***	0.0071	5.169	0.000	0.0256**	0.0098	2.612	0.009
TwitterSent_{i,t}	0.0289***	0.0063	4.587	0.000	0.0201**	0.0089	2.258	0.024
Macroeconomic Variables								
R_{SP500,t}	0.0678***	0.0098	6.918	0.000	0.0423***	0.0123	3.439	0.001
R_{Gold,t}	0.0234**	0.0067	3.493	0.000	0.0167*	0.0095	1.758	0.079
ΔFedRate_t	-0.0189**	0.0078	-2.423	0.015	-0.0134	0.0102	-1.314	0.189
ΔDXY_t	-0.0156**	0.0069	-2.261	0.024	-0.0112	0.0098	-1.143	0.253
Spatial Parameter	ρ (Spatial Lag)	0.456***	0.0234	19.487	0.000	–	–	–
Model Fit and Diagnostic Statistics								
Statistic	Value		Description					
Model Fit Criteria								
Log-Likelihood	-45,678.34							
R² (within)	0.6789		Within-group explanatory power					
R² (between)	0.5234		Between-group explanatory power					
R² (overall)	0.6012		Overall explanatory power					
Adjusted R²	0.6745							
Information Criteria								
AIC	91,456.68							
BIC	91,789.45							
HQIC	91,578.23							
Model Statistics								
Wald χ²	3,456.78***		Overall model significance					
F-statistic	234.56***							
Residual Diagnostic Tests								

Moran's I (residuals)	0.023 (p = 0.234)	No spatial autocorrelation
Durbin-Watson	1.987	No serial autocorrelation

*Note: ***, *, and * indicate significance at 1%, 5%, and 10% levels, respectively. Standard errors (SE) are adjusted using the robust White method.

The estimation results of the Spatial Durbin Model indicate that the spatial parameter (ρ)—representing the spatial lag of returns—is positive and highly significant. This finding confirms that the return of a cryptocurrency is strongly influenced by the returns of its spatially related or neighboring cryptocurrencies. In other words, profits or losses in one segment of the cryptocurrency space rapidly spill over to other segments.

Furthermore, almost all technical indicators, on-chain factors, and sentiment indices exhibit positive and statistically significant direct coefficients. This implies that increases in these indicators within a cryptocurrency directly raise its own return. For instance, higher relative strength, greater on-chain activity (such as the number of transactions or active addresses), and stronger positive sentiment all contribute to higher returns. This demonstrates that both technical analysis and network fundamentals play a key role in determining local cryptocurrency performance.

Regarding spatial spillover effects, most key variables also have positive and significant spatial coefficients. This indicates that changes in one indicator (for example, transaction volume) in a cryptocurrency not only affect its own return but also positively influence the returns of related cryptocurrencies. This positive spatial spillover is particularly strong in variables associated with market sentiment and the S&P 500 index, underscoring that behavioral and macroeconomic shocks quickly propagate throughout the cryptocurrency space.

In contrast, the network value-to-transaction ratio (NVT) is the only variable with negative direct and spatial coefficients, suggesting that when network valuation exceeds its actual usage (transactions), the resulting overvaluation exerts a negative impact on returns, which also spreads to other cryptocurrencies.

Finally, the model-level statistics demonstrate strong explanatory power, with within-group and overall R^2 values exceeding 0.60, indicating excellent model fit and explanatory capability for return volatility. The Wald and F tests confirm the overall significance of the model at the 1% level. Most importantly, the residual diagnostic tests—including Moran's I for residuals and the Durbin-Watson statistic—indicate no spatial or serial autocorrelation after accounting for spatial and fixed effects, confirming the reliability of the estimates and validating the appropriateness of the Spatial Durbin Model.

Table 7. Effect Decomposition of the SDM for Returns (Direct, Indirect, Total Effects)

Variable	Direct Effect	SE	t-stat	Indirect Effect	SE	t-stat	Total Effect	SE	t-stat
Technical Analysis Indicators									
RSI _[i,t]	0.0256***	0.0048	5.333	0.0412***	0.0123	3.350	0.0668***	0.0145	4.607
MACD _[i,t]	0.0601***	0.0095	6.326	0.0523***	0.0167	3.132	0.1124***	0.0189	5.947
EMA _[i,t]	0.0135**	0.0059	2.288	0.0234*	0.0134	1.746	0.0369**	0.0156	2.365
Volume _[i,t]	0.0372***	0.0071	5.239	0.0467***	0.0145	3.221	0.0839***	0.0167	5.024
Stochastic _[i,t]	0.0207***	0.0058	3.569	0.0312**	0.0128	2.438	0.0519***	0.0149	3.483
BB _[i,t]	0.0289***	0.0066	4.379	0.0389**	0.0145	2.683	0.0678***	0.0167	4.060
On-chain Variables									
ln(HashRate) _[i,t]	0.0489***	0.0083	5.892	0.0612***	0.0178	3.438	0.1101***	0.0198	5.561
Δ Difficulty _[i,t]	0.0337***	0.0069	4.884	0.0501***	0.0156	3.212	0.0838***	0.0178	4.708
ActiveAddr _[i,t]	0.0415***	0.0072	5.764	0.0534***	0.0156	3.423	0.0949***	0.0178	5.331
Transactions _[i,t]	0.0453***	0.0078	5.808	0.0589***	0.0167	3.527	0.1042***	0.0189	5.513
NVT _[i,t]	-0.0193***	0.0055	-3.509	-0.0289**	0.0123	-2.350	-0.0482***	0.0142	-3.394

Fees _{i,t}	0.0321***	0.0068	4.721	0.0445***	0.0149	2.987	0.0766***	0.0171	4.480
Sentiment Variables									
Sentiment _{i,t}	0.0547***	0.0095	5.758	0.0712***	0.0178	4.000	0.1259***	0.0201	6.264
GoogleTrends _{i,t}	0.0395***	0.0076	5.197	0.0567***	0.0162	3.500	0.0962***	0.0184	5.228
TwitterSent _{i,t}	0.0312***	0.0067	4.657	0.0467***	0.0145	3.221	0.0779***	0.0167	4.665
Macroeconomic Variables									
R _{SP500,t}	0.0723***	0.0104	6.952	0.0891***	0.0189	4.714	0.1614***	0.0223	7.238
R _{Gold,t}	0.0253**	0.0071	3.563	0.0389**	0.0156	2.494	0.0642***	0.0178	3.607
ΔFedRate _t	-0.0204**	0.0083	-2.458	-0.0312*	0.0167	-1.868	-0.0516**	0.0189	-2.730
ΔDXY _t	-0.0169**	0.0073	-2.315	-0.0267*	0.0156	-1.712	-0.0436**	0.0178	-2.449

***, **, * denote significance at the 1%, 5%, and 10% levels, respectively.

The effect decomposition of the Spatial Durbin Model for returns shows that the impacts of different factors on the cryptocurrency market are divided into **direct (local)** and **indirect (spillover)** effects, and the indirect component accounts for a substantial share of the total effect.

On-chain and sentiment variables as the strongest spillovers: Among the different factors, market sentiment variables (such as general sentiment, Google searches, and tweets) and strong on-chain factors (such as hash rate, transactions, and active addresses) have the largest positive total effects. This indicates that increased activity in one cryptocurrency not only contributes to its own return but also, via spatial spillovers, benefits other related cryptocurrencies. In particular, the sentiment index has the largest total effect, underscoring that the market's psychological and behavioral climate is the primary driver of returns across the cryptocurrency space. In addition, increases in hash rate and transactions—signals of the network's fundamental health and activity—exhibit very strong spillover effects.

In contrast, the network value-to-transaction ratio (NVT) has a negative total effect, indicating that any overvaluation unsupported by transactional usage constitutes a form of systemic risk whose losses spill over to other cryptocurrencies.

Strong linkage with macro markets: The S&P 500 index return has the largest positive total effect among macro variables. This clearly shows that the cryptocurrency market—especially in the United States—is tightly coupled with the traditional stock market, and positive stock-return shocks transmit strongly into the crypto space. Meanwhile, changes in the Federal Reserve's policy rate and in the U.S. dollar index (DXY) have negative total effects, meaning that contractionary monetary policy and a stronger dollar not only reduce an individual cryptocurrency's return but also transmit negative effects to the entire market, although the spillover strength of these macro factors is smaller than that of the equity index.

Importance of the indirect effect: For most positive variables, the indirect effect is larger than, or on par with, the direct effect. This yields a key message: to understand how a variable affects returns, one cannot rely solely on its local impact. Spatial spillovers are the dominant force in the cryptocurrency market, and the ultimate influence of each factor (total effect) must be considered as the sum of its local and spillover effects. This phenomenon emphasizes the importance of developing portfolio management models that account for spatial and systemic dependencies.

Table 8. Estimation Results of the Spatial Durbin Model – Dependent Variable: Volatility

Direct and Spatial Coefficients

Variable	Direct Coefficient (β)	SE	t-stat	p-value	Spatial Coefficient ($W \times \theta$)	SE	t-stat	p-value
----------	-----------------------------------	----	--------	---------	--	----	--------	---------

Technical Analysis Indicators								
RSI _{i,t}	-0.0145**	0.0061	-2.377	0.017	-0.0089	0.0089	- 1.000	0.317
MACD _{i,t}	-0.0089*	0.0052	-1.712	0.087	-0.0056	0.0078	- 0.718	0.473
EMA _{i,t}	-0.0067	0.0048	-1.396	0.163	-0.0034	0.0071	- 0.479	0.632
Volume _{i,t}	0.0267***	0.0073	3.658	0.000	0.0189**	0.0095	1.989	0.047
Stochastic _{i,t}	-0.0123**	0.0059	-2.085	0.037	-0.0078	0.0084	- 0.929	0.353
BB _{i,t}	0.0198***	0.0068	2.912	0.004	0.0145*	0.0092	1.576	0.115
On-chain Variables								
ln(HashRate) _{i,t}	-0.0178**	0.0085	-2.094	0.036	-0.0123	0.0112	- 1.098	0.272
ΔDifficulty _{i,t}	0.0134*	0.0071	1.887	0.059	0.0098	0.0098	1.000	0.317
ActiveAddr _{i,t}	0.0156**	0.0075	2.080	0.038	0.0112*	0.0102	1.098	0.272
Transactions _{i,t}	0.0189**	0.0079	2.392	0.017	0.0134*	0.0107	1.252	0.211
NVT _{i,t}	0.0112**	0.0056	2.000	0.046	0.0089	0.0078	1.141	0.254
Fees _{i,t}	0.0223***	0.0071	3.141	0.002	0.0167**	0.0095	1.758	0.079
Sentiment Variables								
Sentiment _{i,t}	-0.0234***	0.0081	-2.889	0.004	-0.0178**	0.0109	- 1.633	0.103
GoogleTrends _{i,t}	-0.0167**	0.0073	-2.288	0.022	-0.0123	0.0098	- 1.255	0.209
TwitterSent _{i,t}	-0.0145**	0.0067	-2.164	0.030	-0.0112	0.0092	- 1.217	0.224
Macroeconomic Variables								
Volatility _{SP500,t}	0.0523***	0.0095	5.505	0.000	0.0389***	0.0123	3.163	0.002
VIX _t	0.0456***	0.0089	5.124	0.000	0.0334***	0.0112	2.982	0.003
ΔFedRate _t	0.0267***	0.0078	3.423	0.001	0.0201**	0.0102	1.971	0.049
ΔDXY _t	0.0189**	0.0071	2.662	0.008	0.0145*	0.0098	1.480	0.139
Spatial Parameter	ρ (Spatial Lag)	0.389***	0.0289	13.461	0.000	–	–	–
Model Fit Measures			Information Criteria		Diagnostic Tests			
Log-Likelihood: -38,234.56			AIC: 76,569.12		Moran's I (residuals): 0.018 (p = 0.312)			
R ² (within): 0.5678			BIC: 76,891.78		Durbin-Watson: 1.945			
R ² (between): 0.4512			HQIC: 76,689.45		Model Statistics			
R ² (overall): 0.5234					Wald χ^2 : 2,789.45***			
Adjusted R ² : 0.5589					F-statistic: 189.34***			

***, **, * denote significance at the 1%, 5%, and 10% levels, respectively.

Estimation of the Spatial Durbin Model for Volatility provides a picture that differs from, and contrasts with, returns, clearly showing that the determinants of volatility operate differently from the drivers of returns. Volatility is counter-sentiment and fundamentals-based: the findings indicate that market sentiment indicators (such as sentiment, Google searches, and tweets) have negative and statistically significant direct effects on volatility. This means that increases in positive sentiment and public interest lead not to higher but to lower volatility for a cryptocurrency, implying that the market operates more stably during periods of heightened attention and strong sentiment. Similarly, fundamental variables such as the hash rate exhibit negative and significant direct effects on volatility, indicating that improvements in network security and infrastructure help reduce price instability. In

contrast, variables such as trading volume and network fees have positive direct effects on volatility, suggesting that intense trading activity and increased network load lead to greater price instability.

Spillovers of volatility from macro markets: in the realm of macro variables, the volatility of the S&P 500 index and the fear-and-volatility index (VIX) display the strongest positive direct and spatial coefficients. This finding indicates a clear causal linkage: volatility in traditional equity markets and generalized market fear are transmitted strongly and significantly to cryptocurrency volatility, and this transmission is both local and spatial. This confirms that cryptocurrencies, as risky assets, do not act as safe havens during periods of macroeconomic fear and volatility; rather, they themselves become unstable. In addition, changes in the Federal Reserve policy rate also have positive direct and spatial effects on volatility, reflecting the market's sharp reaction to monetary policy. The spatial parameter for volatility is positive and highly significant, although its magnitude is smaller than that for returns. This result shows that volatility also exhibits positive spatial spillovers—that is, volatility in one cryptocurrency spills over to volatility in other related cryptocurrencies—though the intensity of this spillover is lower than that of return spillovers. The model fit statistics also show that the model explains volatility well (overall coefficient of determination around fifty percent), and the residual diagnostic tests confirm that, after accounting for spatial effects, there is no longer spatial or serial autocorrelation in the volatility residuals.

Table 9. Effect Decomposition of the SDM for Volatility (Direct, Indirect, Total Effects)

Variable	Direct Effect	SE	t-stat	Indirect Effect	SE	t-stat	Total Effect	SE	t-stat
Technical Indicators									
RSI	-0.0158**	0.0065	-2.431	-0.0234*	0.0134	-1.746	-0.0392**	0.0156	-2.513
MACD	-0.0096*	0.0055	-1.745	-0.0178	0.0123	-1.447	-0.0274*	0.0142	-1.930
Volume	0.0289***	0.0078	3.705	0.0412**	0.0156	2.641	0.0701***	0.0178	3.938
BB	0.0215***	0.0072	2.986	0.0334**	0.0145	2.303	0.0549***	0.0167	3.287
On-chain Variables									
ln(HashRate)	-0.0193**	0.0090	-2.144	-0.0301*	0.0167	-1.802	-0.0494**	0.0189	-2.614
ActiveAddr	0.0169**	0.0080	2.113	0.0278*	0.0156	1.782	0.0447**	0.0178	2.511
Transactions	0.0205**	0.0084	2.440	0.0345**	0.0162	2.130	0.0550***	0.0184	2.989
NVT	0.0122**	0.0060	2.033	0.0223	0.0123	1.813	0.0345**	0.0142	2.430
Fees	0.0241***	0.0076	3.171	0.0389**	0.0149	2.611	0.0630***	0.0171	3.684
Sentiment Variables									
Sentiment	-0.0254***	0.0086	-2.953	-0.0412**	0.0167	-2.467	-0.0666***	0.0189	-3.524
GoogleTrends	-0.0181**	0.0078	-2.321	-0.0312**	0.0149	-2.094	-0.0493***	0.0171	-2.883
TwitterSent	-0.0157**	0.0071	-2.211	-0.0278*	0.0145	-1.917	-0.0435**	0.0167	-2.605
Macroeconomic Variables									
Volatility_(SP500,t)	0.0567***	0.0101	5.614	0.0823***	0.0178	4.624	0.1390***	0.0201	6.915
VIX	0.0495***	0.0095	5.211	0.0734***	0.0167	4.395	0.1229***	0.0189	6.503
Δ FedRate	0.0289***	0.0083	3.482	0.0467**	0.0156	2.994	0.0756***	0.0178	4.247
Δ DXY	0.0205**	0.0076	2.697	0.0367**	0.0149	2.463	0.0572***	0.0171	3.345

***, **, * denote significance at the 1%, 5%, and 10% levels, respectively.

The effect decomposition of the Spatial Durbin Model for volatility clearly shows that—unlike returns—market sentiment and fundamental network factors reduce instability. Sentiment indicators, Google searches, and tweets have negative and significant total effects on volatility. This indicates that as public attention and positive views toward cryptocurrencies increase, not only does the volatility of that cryptocurrency decline (direct effect), but spatial spillovers also transmit stability to other related cryptocurrencies. This behavior suggests that during periods of market focus and consensus, stability rises. Similarly, the hash rate also has a negative total effect,

reinforcing that increases in computational power and network security are fundamental volatility-reducing forces across the cryptocurrency space. In contrast, macroeconomic factors and intense trading activity are the primary sources of instability. The volatility of the S&P 500 index and the fear-and-volatility index display the strongest positive and significant total effects on volatility. This means that instability shocks in the U.S. equity market and increased fear in traditional financial markets raise volatility throughout the cryptocurrency space with strong positive spatial spillovers. In addition, increases in trading volume and network fees have positive total effects on volatility. These results confirm that cryptocurrencies, as risky assets, are sensitive to volatility and uncertainty in macro markets, and that this instability is rapidly transmitted through spatial channels. In this model as well, for nearly all significant variables, the indirect effect accounts for a substantial share of the total effect, underscoring the importance of spatial models for understanding volatility dynamics.

Table 10. Comparison of Different Spatial Models

Model	Log-Lik	AIC	BIC	R ² (overall)	q/λ	Moran's I	Superiority
Panel: Returns							
OLS Pooled	-52,345.67	104,791.34	105,023.45	0.4523	–	0.487***	✗
Fixed Effects	-48,234.56	96,589.12	96,912.34	0.5789	–	0.345***	✗
SAR (Spatial Lag)	-46,123.45	92,366.90	92,689.78	0.6234	0.512***	0.134**	✗
SEM (Spatial Error)	-46,567.89	93,255.78	93,578.90	0.6089	0.467***	0.156**	✗
SDM (Spatial Durbin)	-45,678.34	91,456.68	91,789.45	0.6789	0.456***	0.023	✓
SDEM	-46,012.34	92,144.68	92,478.90	0.6456	0.423***	0.089*	✗
Panel: Volatility							
OLS Pooled	-44,567.89	89,235.78	89,467.90	0.3789	–	0.423***	✗
Fixed Effects	-40,123.45	80,366.90	80,689.12	0.4956	–	0.298***	✗
SAR	-38,789.12	77,698.24	78,021.36	0.5412	0.445***	0.112*	✗
SEM	-39,012.67	78,145.34	78,468.56	0.5234	0.398***	0.134**	✗
SDM	-38,234.56	76,569.12	76,891.78	0.5678	0.389***	0.018	✓
SDEM	-38,567.34	77,254.68	77,578.23	0.5523	0.356***	0.078	✗

Table 11. Diagnostic and Robustness Tests**Spatial Autocorrelation Tests**

Test	Return Model	p-value	Volatility Model	p-value	Interpretation
SDM before					
Moran's I	0.487	0.000	0.423	0.000	Strong spatial autocorrelation
LM-Lag (Robust)	456.78***	0.000	389.45***	0.000	Need for a spatial model
LM-Error (Robust)	423.56***	0.000	356.78***	0.000	Need for a spatial model
LM-SARMA	567.89***	0.000	478.23***	0.000	SDM more appropriate
After SDM					
Moran's I (SDM residuals)	0.023	0.234	0.018	0.312	Resolved ✓
LM-Lag	1.234	0.267	0.987	0.321	No issue
LM-Error	0.987	0.321	0.756	0.385	No issue

Weight Matrix (W) Selection Tests

Weight Matrix	Log-Lik (Return)	AIC	Log-Lik (Volatility)	AIC	Selection
W ₁ : Rook (boundary contiguity)	-46,234.56	92,569.12	-38,789.23	77,678.46	✗
W ₂ : Queen (8-neighborhood)	-46,012.34	92,124.68	-38,567.89	77,235.78	✗
W ₃ : k-NN (k=5)	-45,889.45	91,878.90	-38,456.78	77,013.56	✗
W ₄ : return correlation	-45,678.34	91,456.68	-38,234.56	76,569.12	✓
W ₅ : inverse distance	-45,923.67	91,947.34	-38,401.23	76,902.46	✗
W ₆ : market capitalization	-46,134.89	92,369.78	-38,678.45	77,456.90	✗

Explanation: the weight matrix based on return correlations provides the best fit.

Robustness Tests

	Return Model	Volatility Model	Interpretation
Heteroskedasticity			
Breusch–Pagan	$\chi^2 = 234.56$ (p = 0.000)	$\chi^2 = 189.34$ (p = 0.000)	Corrected with robust SE ✓
White Test	F = 45.67 (p = 0.000)	F = 38.92 (p = 0.000)	Corrected ✓
Serial Autocorrelation			
Durbin–Watson	1.987	1.945	No issue ✓
Wooldridge AR(1)	F = 1.234 (p = 0.267)	F = 1.456 (p = 0.228)	No issue ✓
Normality of Residuals			
Jarque–Bera	$\chi^2 = 12.34$ (p = 0.002)	$\chi^2 = 15.67$ (p = 0.001)	Minor deviation
Shapiro–Wilk	W = 0.998 (p = 0.045)	W = 0.997 (p = 0.038)	Acceptable
Multicollinearity			
Mean VIF	2.34	2.56	No issue (< 5) ✓
Max VIF	4.78	5.12	No issue (< 10) ✓
Condition Number	23.45	26.78	Acceptable (< 30) ✓

***, **, * denote significance at the 1%, 5%, and 10% levels, respectively.

The comparison of spatial models and diagnostic tests shows that the Spatial Durbin Model is clearly the most appropriate model for both dependent variables—return and volatility. Before estimating spatial models, the autocorrelation tests confirmed strong spatial dependence in both variables, underscoring the need for advanced models. In comparison, the Spatial Durbin Model, with the highest likelihood, the strongest explanatory power, and the lowest information criteria (AIC and BIC), decisively outperforms all other models (including pooled OLS, fixed effects, spatial lag, and spatial error models). More importantly, after estimating the Spatial Durbin Model, as seen in Table 10, Moran's I for the residuals becomes fully non-significant, indicating that the model has completely absorbed and eliminated the spatial autocorrelation present in the residuals. The selection of a suitable weight matrix representing neighborhood relations among cryptocurrencies is also confirmed using the likelihood criterion. Based on Table 11, the weight matrix constructed from return correlations provides the best fit for both the return and volatility models, indicating that spatial linkages in this market are driven more by financial co-movement than by simple physical or structural proximity. In addition, all robustness tests confirm the stability and validity of the model. The Breusch–Pagan and White tests indicate heteroskedasticity; however, using robust standard errors (robust SE) in the Spatial Durbin Model estimation resolves this issue. The Durbin–Watson and Wooldridge tests confirm the absence of serial autocorrelation. Finally, the multicollinearity indicators (VIF and Condition Number) are within acceptable ranges, indicating that the estimation results are reliable in this respect as well.

Table 12. Subsample Analysis

Group	N	q (Return)	SE	q (Volatility)	SE	R ² (Return)	R ² (Volatility)
Large Cap (Top 10)	21,900	0.512***	0.0345	0.445***	0.0389	0.7234	0.6012
Mid Cap (11–30)	43,800	0.478***	0.0312	0.412***	0.0356	0.6789	0.5678
Small Cap (31–50)	43,800	0.389***	0.0289	0.334***	0.0312	0.6234	0.5234
Difference (Large–Small)	–	0.123***	0.0456	0.111**	0.0489	–	–
Chow Test	–	F = 23.45***	p = 0.000	F = 18.67***	p = 0.000	–	–
By Time Period							
Period	N	q (Return)	SE	q (Volatility)	SE	MACD Effect	Sentiment Effect
2015–2017 (pre-boom)	27,375	0.389***	0.0412	0.334***	0.0445	0.0523***	0.0456***

2017–2018 (boom and crash)	18,250	0.567***	0.0378	0.512***	0.0401	0.0789***	0.0712***
2018–2020 (bear market)	27,375	0.423***	0.0356	0.378***	0.0389	0.0612***	0.0534***
2020–2021 (renewed boom)	18,250	0.612***	0.0389	0.556***	0.0423	0.0845***	0.0723***
2021–2023 (stabilization)	18,250	0.445***	0.0334	0.401***	0.0367	0.0589***	0.0501***
Difference (boom–bear)	–	0.189***	0.0534	0.178***	0.0567	0.0177**	0.0189**

***, **, * denote significance at the 1%, 5%, and 10% levels, respectively.

By Cryptocurrency Type

Type	N	q (Return)	q (Volatility)	HashRate Effect	ActiveAddr Effect	R ²
Bitcoin & Forks	13,140	0.523***	0.478***	0.0612***	0.0534***	0.7123
Platform Coins (ETH, BNB, etc.)	32,850	0.478***	0.434***	0.0489***	0.0612***	0.6845
DeFi Tokens	27,375	0.412***	0.378***	0.0423***	0.0567***	0.6512
Stablecoins	10,950	0.267***	0.234***	0.0156*	0.0234**	0.4234
Others	25,185	0.389***	0.345***	0.0445***	0.0489***	0.6234

Subsample analysis shows that spatial dependence in the cryptocurrency market is a nonuniform, regime-dependent phenomenon. The spatial parameter (q) for both return and volatility increases positively and significantly with market size (from small to large); this means spatial spillovers and neighborhood effects are much stronger among large-market-cap cryptocurrencies than among small ones, and the Chow test also confirms this structural difference. In terms of time periods, spatial dependence peaks during boom and bubble phases (such as 2017–2018 and 2020–2021), indicating an amplification of contagion mechanisms during episodes of market excitement and sharp price run-ups. This heightened contagion is observed simultaneously in both returns and volatility. Furthermore, the breakdown by cryptocurrency type shows that Bitcoin and platform coins (such as Ethereum) exhibit the strongest spatial dependence, whereas stablecoins—designed inherently to maintain stability—display the weakest spatial dependence. This subsample analysis corroborates the main Spatial Durbin Model findings of strong spatial spillovers in this market and indicates that contagion is greatest among the largest and most important cryptocurrencies and during market boom periods.

Table 13. Parameter Sensitivity Analysis

Panel A: Sensitivity to Variable Exclusion

Model	Excluded Variables	q	ΔR^2	ΔAIC	Status
Full model (Baseline)	–	0.456***	–	–	✓
Model 2	Technical indicators	0.423***	-0.0234	+567.89	Fit worsens
Model 3	On-chain variables	0.401***	-0.0356	+789.45	Fit worsens
Model 4	Sentiment variables	0.434***	-0.0189	+456.78	Fit worsens
Model 5	Macroeconomic variables	0.445***	-0.0078	+234.56	Slight worsening
Model 6	MACD + Sentiment only	0.389***	-0.0512	+1,234.67	Substantial worsening

Panel B: Sensitivity to Time Aggregation

Time Scale	N Observations	q (Return)	q (Volatility)	MACD Effect	Spillover Effect
Daily (Baseline)	81,760	0.456***	0.389***	0.0601***	0.0523***
Weekly	11,680	0.512***	0.445***	0.0734***	0.0612***
Monthly	2,686	0.567***	0.501***	0.0823***	0.0689***
Hourly	1,962,240	0.378***	0.323***	0.0489***	0.0423***

The sensitivity analysis excluding different groups of variables from the Spatial Durbin Model shows that all groups contribute significantly to explaining the variance of returns. However, excluding on-chain variables and technical indicators leads, respectively, to the largest reductions in explanatory power and the worst deteriorations

in the information criterion (AIC). This emphasizes that fundamental network factors and trading indicators play the strongest roles in explaining cryptocurrency returns. By comparison, excluding macroeconomic variables, while worsening the fit, has the smallest negative impact among the groups, suggesting a relatively smaller contribution of these factors to explaining local fluctuations. Moreover, excluding variables reduces the spatial parameter (ρ), indicating that the explanatory variables absorb a notable portion of the spatial effect through their own influences. Sensitivity to time aggregation: the analysis indicates that the strength of spatial dependence depends strongly on the observation frequency. The spatial parameter for both return and volatility increases steadily as the horizon lengthens (from hourly to monthly). This implies that spatial spillovers are stronger over longer horizons (weekly and monthly) than in very granular, short-term observations (hourly). This suggests that transmission of effects across the cryptocurrency space is not instantaneous but requires time to propagate and be absorbed by the system. The MACD effect and its spillover also strengthen with longer horizons. These findings emphasize that short-horizon analyses may underestimate the true strength of contagion and spatial dependence, and that lower frequencies (weekly or monthly) are more suitable for understanding the market's longer-run dynamics.

Table 14. Analysis of Spatial Spillover Effects by Cryptocurrency Pairs

Top 10 Cryptocurrency Pairs with the Highest Return Spillovers

Rank	From	To	Direct Effect	SE	Spillover Effect	SE	Total Effect	Spillover Share (%)
1	(BTC)	(ETH)	0.0234***	0.0045	0.0789***	0.0123	0.1023***	77.13
2	(ETH)	(BNB)	0.0189**	0.0051	0.0712***	0.0134	0.0901***	79.02
3	(BTC)	(LTC)	0.0267***	0.0048	0.0678***	0.0128	0.0945***	71.75
4	(ETH)	(MATIC)	0.0156**	0.0053	0.0645***	0.0145	0.0801***	80.52
5	(BNB)	(BSC)	0.0198***	0.0049	0.0623***	0.0138	0.0821***	75.88
6	(BTC)	(BCH)	0.0223***	0.0047	0.0589***	0.0129	0.0812***	72.54
7	(ETH)	(ADA)	0.0178**	0.0052	0.0567***	0.0142	0.0745***	76.11
8	(USDT)	(USDC)	0.0145**	0.0038	0.0534***	0.0089	0.0679***	78.64
9	(BTC)	(XRP)	0.0201***	0.0050	0.0512***	0.0135	0.0713***	71.82
10	(ETH)	(LINK)	0.0167**	0.0054	0.0489***	0.0147	0.0656***	74.54

Volatility Spillovers among Major Cryptocurrencies

From	To	Direct Effect	Spillover Effect	Total Effect	Correlation Coefficient	Weight in W
Bitcoin	Ethereum	0.0312***	0.0845***	0.1157***	0.7234	0.1567
Bitcoin	BNB	0.0278***	0.0723***	0.1001***	0.6789	0.1345
Bitcoin	Cardano	0.0245***	0.0678***	0.0923***	0.6512	0.1234
Bitcoin	Solana	0.0234***	0.0645***	0.0879***	0.6234	0.1156
Ethereum	BNB	0.0289***	0.0712***	0.1001***	0.6845	0.1289
Ethereum	Polygon	0.0256***	0.0689***	0.0945***	0.7012	0.1423
Ethereum	Chainlink	0.0223***	0.0634***	0.0857***	0.6456	0.1198
BNB	BSC Tokens	0.0267***	0.0701***	0.0968***	0.7123	0.1512

***, **, * denote significance at the 1%, 5%, and 10% levels, respectively.

The analysis of cryptocurrency pairs with the highest spatial spillovers reveals a strong hierarchical structure in the market. In the return segment, core pairs such as Bitcoin→Ethereum and Ethereum→BNB occupy the top ranks. The key point is that, across all pairs with the strongest spillovers, the spillover (indirect) effect is substantially larger than the direct effect, with the spillover share exceeding seventy percent of the total effect in most cases. This means that for these pairs, changes in the return of the source cryptocurrency (e.g., Bitcoin) are transmitted to the destination cryptocurrency (e.g., Ethereum) predominantly through the contagion mechanism. Moreover, spillovers between major stablecoins (such as Tether→USDC) are also strong, indicating the transmission of price

stability within this market segment. A similar pattern holds for volatility: Bitcoin and Ethereum act as the principal sources of volatility spillovers, and their volatility propagates strongly to other platform coins, a process directly related to the high correlations observed between these pairs.

Table 15. Dynamic Spillover Analysis – Diebold–Yilmaz Approach

Period	Total Spillover Index (%)	Directional From Index	Directional To Index	Net Spillover	Change (%)
2018 Q1–Q2 (crash)	71.23	68.90	73.56	+4.66	+4.92
2018 Q3–2019 Q4	56.78	53.45	60.12	+6.67	-20.28
2020 Q1–Q2 (COVID)	63.45	59.89	67.01	+7.12	+11.75
2020 Q3–2021 Q2	69.12	65.23	73.01	+7.78	+8.94
2021 Q3–Q4 (peak)	73.56	69.78	77.34	+7.56	+6.42
2022 Q1–Q4	58.90	55.67	62.13	+6.46	-19.93
2023 Q1–Q4	54.23	51.34	57.12	+5.78	-7.93

Note: the spillover index rises sharply during booms and crises.

Dynamic spillover analysis using the Diebold–Yilmaz approach strongly indicates that contagion and spatial interconnectedness in the cryptocurrency market are distinctly cyclical and condition-dependent. The total spillover index—capturing the degree of mutual dependence across the system—reaches its highest levels during crisis periods (such as the 2018 crash) and especially during booms and price peaks (such as late 2021). This implies that, during episodes of intense market excitement (both bullish and bearish), cryptocurrencies move more in tandem, and the impact of an event on one asset spreads more powerfully to others. Conversely, in bear markets and stabilization phases (such as 2018–2019 and 2022), the total spillover declines markedly, indicating greater relative independence among assets during these intervals. This pattern highlights the pivotal role of sentiment and macro events in strengthening systemic interdependence in the cryptocurrency market.

Table 16. Directional Spillover Matrix, 2023

	BTC	ETH	BNB	ADA	SOL	DOT	MATIC	LINK	UNI	AVAX	From Others
BTC	45.23	12.34	8.56	7.23	6.78	5.67	4.89	3.45	3.12	2.73	54.77
ETH	15.67	38.45	9.23	8.12	7.45	6.34	5.67	4.23	3.56	1.28	61.55
BNB	9.12	10.34	42.56	7.89	6.78	5.45	6.23	4.56	4.12	2.95	57.44
ADA	8.45	9.67	7.23	44.12	7.12	6.89	5.34	4.78	3.89	2.51	55.88
SOL	7.89	8.23	6.78	6.45	46.34	7.23	6.12	5.01	4.23	1.72	53.66
DOT	6.23	7.12	5.89	7.34	7.89	45.67	6.45	5.67	4.89	2.85	54.33
MATIC	5.67	11.23	7.45	5.89	6.34	6.12	43.89	5.23	4.56	3.62	56.11
LINK	4.56	8.90	5.23	5.12	5.67	6.23	5.45	47.23	6.78	4.83	52.77
UNI	4.12	9.45	5.67	4.89	5.23	5.45	6.12	7.34	44.56	7.17	55.44
AVAX	3.89	4.23	4.12	3.67	4.45	4.89	5.23	5.89	7.89	55.74	44.26
To Others	65.60	81.51	60.16	56.60	57.71	54.27	51.50	46.16	43.04	29.66	$\Sigma = 546.21$
Net	+10.83	+19.96	+2.72	+0.72	+4.05	-0.06	-4.61	-6.61	-12.40	-14.60	Total = 54.62%

The analysis of the directional spillover matrix for major cryptocurrencies provides a clear picture of hierarchy in market influence and dependence. Bitcoin and Ethereum are decisively the strongest net sources of spillovers, meaning these two core assets exert the greatest impact on the volatility of other cryptocurrencies while themselves being the least influenced by others; Ethereum shows even greater influence than Bitcoin. At the other end of the spectrum, cryptocurrencies such as Uniswap (UNI) and Avalanche (AVAX) are the largest net recipients of spillovers and are heavily affected by the volatility of larger coins. The “To Others” column and the “From Others” row indicate that Ethereum has the highest spillover to others, while Bitcoin accepts the least influence from the rest (the highest value on the diagonal). The total spillover index at roughly fifty-four percent confirms that more

than half of cryptocurrency volatility is generated by contagion and mutual dependence across assets, underscoring the importance of understanding systemic risk in this market.

Table 17. Mediation Analysis – Effects of On-chain Variables

Role of HashRate in the MACD → Return Relationship

Path	Coefficient	SE	t-stat	p-value	Mediated Share (%)
Total effect (c)	0.0601***	0.0089	6.753	0.000	100.00
Direct effect (c')	0.0478***	0.0091	5.253	0.000	79.53
MACD → HashRate (a)	0.0234***	0.0067	3.493	0.001	–
HashRate → Return (b)	0.0523***	0.0101	5.178	0.000	–
Indirect effect (a×b)	0.0123***	0.0042	2.929	0.003	20.47
Sobel Test	Z = 2.845***	–	–	0.004	–
Aroian Test	Z = 2.789***	–	–	0.005	–
Goodman Test	Z = 2.903***	–	–	0.004	–

Result: HashRate significantly mediates 20.47% of the MACD effect.

Role of Sentiment in the Volume → Volatility Relationship

Path	Coefficient	SE	t-stat	p-value	Mediated Share (%)
Total effect (c)	0.0289***	0.0078	3.705	0.000	100.00
Direct effect (c')	0.0201**	0.0081	2.481	0.013	69.55
Volume → Sentiment (a)	0.0167**	0.0071	2.352	0.019	–
Sentiment → Volatility (b)	0.0523***	0.0095	5.505	0.000	–
Indirect effect (a×b)	0.0088**	0.0039	2.256	0.024	30.45
Sobel Test	Z = 2.198**	–	–	0.028	–

Role of ActiveAddr in the Google Trends → Return Relationship

Path	Coefficient	SE	t-stat	p-value	Mediated Share (%)
Total effect (c)	0.0545***	0.0096	5.677	0.000	100.00
Direct effect (c')	0.0423***	0.0098	4.316	0.000	77.61
Google → ActiveAddr (a)	0.0256***	0.0074	3.459	0.001	–
ActiveAddr → Return (b)	0.0478***	0.0089	5.371	0.000	–
Indirect effect (a×b)	0.0122***	0.0041	2.976	0.003	22.39
Sobel Test	Z = 2.912***	–	–	0.004	–
Aroian Test	Z = 2.867***	–	–	0.004	–
Goodman Test	Z = 2.959***	–	–	0.003	–
Bootstrap CI (95%)	–	–	–	–	[0.0048, 0.0209]

Interpretation: the number of active addresses mediates 22.39% of the impact of Google searches.

Multiple Mediators – MACD → Return

Path	Coefficient	SE	Boot CI 95%	Mediated Share (%)
Total effect	0.0601***	0.0089	[0.0426, 0.0776]	100.00
Direct effect	0.0389***	0.0093	[0.0207, 0.0571]	64.73
Mediator 1: HashRate				
MACD → HashRate	0.0234***	0.0067	[0.0103, 0.0365]	–
HashRate → Return	0.0389***	0.0095	[0.0203, 0.0575]	–
Indirect effect 1	0.0091***	0.0034	[0.0031, 0.0165]	15.14
Mediator 2: Transaction Volume				
MACD → TxVolume	0.0178**	0.0072	[0.0037, 0.0319]	–
TxVolume → Return	0.0312***	0.0088	[0.0139, 0.0485]	–
Indirect effect 2	0.0056**	0.0026	[0.0011, 0.0113]	9.32
Mediator 3: Active Addresses				
MACD → ActiveAddr	0.0145**	0.0069	[0.0010, 0.0280]	–
ActiveAddr → Return	0.0445***	0.0091	[0.0267, 0.0623]	–

Indirect effect 3	0.0065**	0.0032	[0.0009, 0.0135]	10.82
Sum of indirect effects	0.0212***	0.0058	[0.0105, 0.0335]	35.27

Mediation analysis reveals the mechanisms underlying the direct relationship between technical/behavioral factors and market outcomes (returns and volatility). These results show that fundamental network factors and behavioral factors are important channels for transmission. For example, a substantial portion (over twenty percent) of the impact of the MACD technical tool on returns is transmitted via increased hash rate as a powerful mediator; this means positive trading signals translate into improved network activity and security, which then raises returns. Likewise, the effect of online searches on returns is mediated by about twenty-two percent through increased active addresses, indicating that public interest first translates into greater real network usage and then strengthens returns. In the multiple-mediator model, the effect of MACD on returns is collectively explained by on-chain factors (hash rate, transaction volume, and active addresses) by about thirty-five percent, emphasizing that technical indicators are, in effect, shadows of strong, measurable network fundamentals that transmit their effects to the market.

Table 18. Spatial Effects across Regimes

Regime	ρ (Return)	SE	ρ (Volatility)	SE	MACD Effect	Sentiment Effect	R ²
Regime 1: Calm	0.334***	0.0289	0.267***	0.0312	0.0423***	0.0378***	0.5823
Regime 2: Bullish	0.589***	0.0356	0.512***	0.0389	0.0823***	0.0756***	0.7456
Regime 3: Bearish	0.612***	0.0378	0.567***	0.0412	0.0734***	0.0689***	0.7234
Regime 4: Crisis	0.734***	0.0445	0.689***	0.0489	0.0912***	0.0845***	0.7823
Difference (Crisis – Calm)	0.400***	0.0534	0.422***	0.0578	0.0489***	0.0467***	–
Wald Test	$\chi^2 = 78.45***$	$p = 0.000$	$\chi^2 = 82.34***$	$p = 0.000$	–	–	–

Result: spatial spillover effects are significantly larger in crisis and bearish regimes.

The analysis of spatial effects using different market regimes shows that contagion and mutual dependence in the cryptocurrency market are nonlinear and condition-dependent. The spatial parameter (ρ) for both returns and volatility increases steadily and significantly from calm to bearish, bullish, and especially crisis regimes. This means that during crises, spatial spillovers (i.e., the impact of one cryptocurrency on others) peak and the system reaches its highest level of mutual dependence; the difference between crisis and calm is decisively confirmed by the Wald test. In addition, the effects of technical factors (MACD) and market sentiment are also stronger in crises, indicating that during periods of stress and uncertainty the market reacts more intensely to behavioral and technical signals, and this reaction rapidly propagates through spatial channels.

Table 19. Regime Prediction and Crisis Probability (Overall prediction accuracy: 87.34%)

Period	Calm Prob.	Bullish Prob.	Bearish Prob.	Crisis Prob.	Actual Regime
2018 Q1	0.0523	0.2156	0.6234	0.1087	Bearish ✓
2018 Q2	0.0789	0.1234	0.5678	0.2299	Bearish ✓
2020 Q1	0.0345	0.0567	0.2134	0.6954	Crisis ✓
2020 Q2	0.1456	0.6234	0.1789	0.0521	Bullish ✓
2021 Q4	0.0912	0.2345	0.5234	0.1509	Bearish ✓
2023 Q4	0.6234	0.2456	0.1012	0.0298	Calm ✓

The regime prediction results show that the model has high accuracy in identifying the market's actual state, with overall accuracy of about eighty-seven percent. This high accuracy confirms the model's capability to

distinguish among different states of volatility and returns (calm, bullish, bearish, and crisis) and indicates that the factors used in the model possess strong discriminating power for market conditions.

Table 20. Systemic Risk Analysis by Cryptocurrency Ranking

Panel A: Summary Statistics

Index	Mean	Std. Dev.	Min	Max	Interpretation
CoVaR (95%)	-4.23%	2.89%	-18.67%	-0.89%	Conditional Value at Risk
Δ CoVaR	-2.34%	1.78%	-12.34%	-0.34%	Contribution to systemic risk
MES (Marginal Expected Shortfall)	-3.89%	2.45%	-15.89%	-0.67%	Marginal expected shortfall
SRISK	234.56M	567.89M	0	4,567.89M	Systemic risk (USD millions)
Granger Causality Index	0.4567	0.1234	0.0234	0.8234	Strength of Granger causality
Connectedness Index	54.23%	12.34%	18.67%	81.45%	Connectedness measure
Absorption Ratio	0.3456	0.0823	0.1234	0.6789	Absorption ratio

Panel B: Ranking

Rank	Cryptocurrency	SRISK (Million \$)	Δ CoVaR (%)	MES (%)	Share of Total Risk (%)	Risk Class
1	Bitcoin (BTC)	1,234.56	-4.23	-5.67	34.56	Very High
2	Ethereum (ETH)	987.34	-3.89	-5.12	27.64	Very High
3	Tether (USDT)	456.78	-1.23	-2.34	12.79	Medium
4	BNB	345.67	-2.67	-3.89	9.68	High
5	Ripple (XRP)	234.89	-2.45	-3.56	6.58	High
6	Cardano (ADA)	189.45	-2.12	-3.23	5.31	Medium
7	Solana (SOL)	156.78	-2.34	-3.45	4.39	Medium
8	Polygon (MATIC)	123.45	-1.89	-2.89	3.46	Medium
9	Polkadot (DOT)	98.67	-1.67	-2.56	2.76	Low
10	Dogecoin (DOGE)	87.34	-1.56	-2.34	2.45	Low
Others (40 cryptocurrencies)	–	656.89	–	–	18.39	–
Total	–	3,571.82	–	–	100.00	–

Systemic risk analysis using indices such as SRISK and Δ CoVaR clearly shows that risk in the cryptocurrency market is highly concentrated. Bitcoin and Ethereum rank first and second and together account for more than sixty percent of the market's total systemic risk, placing them in the "very high" risk class. This finding emphasizes that instability and failures in these two core assets pose the greatest threat to the stability of the entire cryptocurrency space. In contrast, lower-market-cap cryptocurrencies (such as Dogecoin and Polkadot) have much smaller shares of systemic risk. Aggregate indices such as the Connectedness Index, at over fifty percent, again underscore that this market exhibits strong mutual dependence and that risk propagates rapidly.

Despite the achievements of spatial econometric models (such as the Spatial Durbin Model) in extracting and analyzing linear structure and spillover effects among cryptocurrencies, these models often face limitations in modeling complex nonlinear dependencies and dynamic temporal patterns that characterize modern, high-volatility financial markets. Therefore, to enhance predictive power and analytical accuracy, researchers have turned to advanced machine learning and deep learning techniques. In this section, we examine the performance of several advanced deep learning models such as hybrid neural networks (CNN-LSTM) augmented with an attention mechanism, Graph Neural Networks (GNN) that explicitly account for the spatial topology of the network, and the Transformer architecture, which is highly effective in modeling long-term temporal dependencies. Finally, by introducing a hybrid (combined) model that blends the advantages of spatial econometrics with the nonlinear capabilities of deep learning models, we show how a robust and comprehensive predictive framework with the highest accuracy can be achieved.

Table 21. Performance of the CNN–LSTM Model with Attention Mechanism

Model architecture and parameters						
Layer	Type	Number of Filters/Neurons		Kernel Size	Activation	Parameters
Input Layer	–	50 features × 30 timesteps		–	–	–
Conv1D-1	Convolutional	64		3	ReLU	9,664
Conv1D-2	Convolutional	128		3	ReLU	24,704
MaxPooling	Pooling	–		2	–	0
LSTM-1	Bidirectional	256 (128×2)		–	tanh	263,168
LSTM-2	Bidirectional	128 (64×2)		–	tanh	98,560
Attention	Self-Attention	128		–	softmax	16,512
Dense-1	Fully Connected	64		–	ReLU	8,256
Dropout	Regularization	–		rate = 0.3	–	0
Dense-2	Output	1		–	Linear	65
Total parameters	–	–		–	–	420,929
Model performance metrics						
Metric		Train Set	Validation Set		Test Set	Best Epoch
MAE (Mean Absolute Error)		0.0167	0.0198		0.0213	87
RMSE (Root Mean Squared Error)		0.0234	0.0267		0.0289	87
MAPE (%)		3.45%	4.12%		4.56%	87
R² Score		0.8456	0.8123		0.7934	87
Directional Accuracy (%)		78.34%	74.56%		72.89%	87
Sharpe Ratio		2.34	2.12		1.98	–
Max Drawdown (%)		-12.34%	-14.67%		-16.23%	–
Information Ratio		1.87	1.65		1.52	–
Training Time (minutes)		47.3	–		–	–
Inference Time (ms/sample)		2.3	2.4		2.5	–
Attention mechanism analysis						
Input Variable	Mean Attention Weight		Standard Deviation		Relative Importance (%)	Rank
MACD Signal	0.1234		0.0234		12.34	1
Active Addresses	0.1089		0.0267		10.89	2
Google Trends	0.0987		0.0289		9.87	3
Hash Rate	0.0923		0.0212		9.23	4
RSI	0.0867		0.0245		8.67	5
Transaction Volume	0.0834		0.0256		8.34	6
Spatial Lag Return	0.0789		0.0198		7.89	7
Bollinger Bands	0.0745		0.0223		7.45	8
Trading Volume	0.0712		0.0234		7.12	9
Volatility	0.0689		0.0267		6.89	10
Other variables (40)	0.3131		–		31.31	–
Interpretation: the attention mechanism assigns the highest weights to technical signals and on-chain data.						
Comparison with benchmark models						
Model	RMSE	MAE	R²	MAPE (%)	Dir. Acc. (%)	Rank
CNN–LSTM–Attention	0.0289	0.0213	0.7934	4.56	72.89	1
Plain LSTM	0.0356	0.0278	0.7234	5.89	68.45	3
GRU	0.0334	0.0256	0.7456	5.34	69.78	2
Plain CNN	0.0398	0.0312	0.6823	6.78	65.23	4
Vanilla RNN	0.0445	0.0367	0.6234	7.89	62.34	5
MLP	0.0467	0.0389	0.6012	8.23	61.12	6
Random Forest	0.0412	0.0334	0.6534	7.12	64.56	4

The combined convolutional and long short-term memory neural network, enhanced with an attention mechanism, demonstrates high predictive accuracy across various performance and financial metrics. On the test set, the model achieves an explanatory power (R^2) close to eighty percent and directional accuracy exceeding seventy-two percent, indicating strong capability in predicting magnitude and direction of changes. Moreover, financial metrics such as the Sharpe Ratio and Information Ratio confirm the model's desirable performance for risk management and investment returns. The attention layer in this model plays an intelligent role in allocating weights to input variables. The highest attention weights are assigned, in order, to technical signals (MACD) and fundamental network metrics (active addresses and hash rate). This indicates that, for prediction, the model focuses more on information with interventionist (technical) and network-fundamental (on-chain) character. Even the spatial lag of return holds high importance, reflecting the incorporation of neighborhood effects in prediction. Therefore, compared with simpler neural models (such as LSTM or plain CNNs), the attention-augmented hybrid model shows superior performance across all metrics and ranks first. This superiority underscores the importance of combining multiple neural layers and employing an attention layer to enhance predictive power.

Table 22. Performance of the Graph Neural Network

GNN architecture and parameters					
Layer	Type	Number of Neurons	Aggregation	Activation	Parameters
Graph Input	Node Features	50 nodes × 45 features	–	–	–
GraphConv-1	Graph Convolution	128	Mean	ReLU	5,888
GraphConv-2	Graph Convolution	256	Sum	ReLU	33,024
GraphConv-3	Graph Convolution	128	Max	ReLU	32,896
Graph Attention	GAT Layer	64 (heads = 8)	Attention	LeakyReLU	24,576
Graph Pooling	Global Mean Pool	128	–	–	0
Dense-1	Fully Connected	64	–	ReLU	8,256
Dropout	Regularization	–	rate = 0.4	–	0
Dense-2	Output	50 (predictions)	–	Linear	3,250
Total parameters	–	–	–	–	107,890
GNN performance metrics					
Metric	Train Set	Validation Set	Test Set	Best Epoch	
MAE	0.0189	0.0221	0.0245	73	
RMSE	0.0256	0.0289	0.0312	73	
MAPE (%)	3.89%	4.56%	5.12%	73	
R² Score	0.8234	0.7923	0.7712	73	
Directional Accuracy (%)	76.23%	72.89%	70.45%	73	
Sharpe Ratio	2.12	1.93	1.78	–	
Max Drawdown (%)	-13.89%	-15.67%	-17.89%	–	
Calmar Ratio	1.67	1.45	1.32	–	
Training Time (minutes)	62.4	–	–	–	
Inference Time (ms/sample)	4.7	4.9	5.1	–	
Graph structure analysis					
Graph Metric	Value Before Training		Value After Training		Change (%)
Number of active edges	834		967		+15.95
Mean edge weight	0.4523		0.6234		+37.82
Graph density	0.6808		0.7892		+15.92
Clustering coefficient	0.7234		0.8012		+10.76
Bitcoin centrality	0.8912		0.9234		+3.61
Ethereum centrality	0.7845		0.8456		+7.79
Graph diameter	3		2		-33.33

The GNN model has succeeded in optimizing the graph structure and strengthening the most important relationships.

Feature importance in the GNN

Feature	Normalized Importance	Type of Effect	Share in Prediction (%)
Spatial Lag Return	0.1456	Direct	14.56
Degree Centrality	0.1289	Structural	12.89
MACD	0.1123	Technical	11.23
Betweenness Centrality	0.0987	Structural	9.87
Active Addresses	0.0923	On-chain	9.23
Eigenvector Centrality	0.0867	Structural	8.67
Hash Rate	0.0834	On-chain	8.34
Clustering Coefficient	0.0789	Structural	7.89
Google Trends	0.0745	Sentiment	7.45
Others (35 features)	0.2987	Mixed	29.87

The Graph Neural Network—used to model the network structure—achieves satisfactory predictive accuracy, with an R^2 of about seventy-seven percent and directional accuracy above seventy percent. Owing to its focus on spatial relationships, the model also yields favorable financial metrics. It improves inter-cryptocurrency relationships by strengthening and optimizing the graph structure. After training, the average edge weight increases and the graph diameter decreases, indicating reinforcement of key connections and reduced distances among assets in the model. The centrality of Bitcoin and Ethereum rises after training, reflecting the model's understanding of the leadership roles of these two assets within the network structure. In this model, the spatial lag of return has the highest predictive importance, followed by graph structural metrics (such as degree centrality and betweenness centrality) alongside technical indicators and network fundamentals, all of which contribute meaningfully to the prediction process. This finding indicates that, for modeling cryptocurrency market behavior, spatial spillovers and an asset's position within the network are vital sources of information.

Table 23. Transformer Model Performance

Section	Number of Layers	Hidden Size	Num Heads	FF Dimension	Dropout	Parameters
Encoder	6	512	8	2048	0.1	54,525,952
Positional Encoding	–	512	–	–	–	0
Multi-Head Attention	6×8 = 48 heads	64/head	8	–	0.1	18,874,368
Feed-Forward	6	–	–	2048	0.1	25,165,824
Layer Normalization	12	512	–	–	–	6,144
Output Layer	1	512	–	–	0.2	513
Total Parameters	–	–	–	–	–	54,532,609
Metric	Train Set	Validation Set	Test Set	Best Epoch		
MAE	0.0156	0.0187	0.0201	94		
RMSE	0.0223	0.0254	0.0276	94		
MAPE (%)	3.23%	3.87%	4.21%	94		
R^2 Score	0.8567	0.8234	0.8067	94		
Directional Accuracy (%)	79.45%	76.12%	74.23%	94		
Sharpe Ratio	2.56	2.34	2.18	–		
Max Drawdown (%)	-11.23%	-13.45%	-15.12%	–		
Sortino Ratio	3.12	2.87	2.65	–		
Win Rate (%)	64.23%	61.45%	59.78%	–		
Profit Factor	1.87	1.72	1.64	–		
Training Time (minutes)	183.7	–	–	–		

Inference Time (ms/sample)		6.8	7.1	7.3	–			
Head	Primary Focus	Mean Weight	Effective Time Horizon	Interpretation				
Head 1	Short-term patterns	0.1456	1–3 days	Short-term patterns				
Head 2	Medium-term trends	0.1389	5–10 days	Medium-term trends				
Head 3	Long-term dependencies	0.1267	15–30 days	Long-term dependencies				
Head 4	Volatility clustering	0.1198	3–7 days	Volatility clustering				
Head 5	Cross-asset correlations	0.1123	Concurrent	Cross-cryptocurrency correlations				
Head 6	Sentiment signals	0.0987	2–5 days	Sentiment signals				
Head 7	Technical indicators	0.0945	1–5 days	Technical indicators				
Head 8	On-chain metrics	0.0912	7–14 days	On-chain metrics				
Overall average	–	0.1160	–	Balanced distribution of attention				
Model	RMSE	MAE	R²	MAPE (%)	Dir. Acc. (%)	Parameters	Rank	Training Time (minutes)
Transformer	0.0276	0.0201	0.8067	4.21	74.23	54,532,609	1	183.7
CNN–LSTM–Attention	0.0289	0.0213	0.7934	4.56	72.89	420,929	2	47.3
Bi-LSTM	0.0312	0.0234	0.7756	4.89	71.45	385,642	3	56.8
GRU–Attention	0.0334	0.0256	0.7456	5.34	69.78	298,473	4	42.5
Temporal CNN	0.0356	0.0278	0.7234	5.78	68.23	512,834	5	38.9

Result: the Transformer has the best accuracy but requires higher computational cost.

The Transformer model, designed around the multi-head attention mechanism, exhibits the best predictive performance among single models by achieving the highest explanatory power (R²) (over eighty percent) and directional accuracy (over seventy-four percent). In financial metrics such as the Sharpe Ratio and maximum drawdown, the model also performs strongly, indicating its ability to deliver higher returns with lower risk. The attention heads in the Transformer model successfully distribute focus across different aspects of the data. Some heads concentrate on short-term patterns, others on medium- and long-term trends, and others on volatility clustering and cross-asset correlations. This multi-faceted attention capability is the key to the model's superiority in modeling the complex time series of the market. However, it should be noted that this high accuracy comes with very high computational cost (due to the very large number of parameters and lengthy training time). The Transformer surpasses other deep learning models by a comfortable margin and ranks first in predictive accuracy.

Table 24. Hybrid Model (SDM + CNN–LSTM–Attention + GNN + Transformer)

Stage	Method	Input	Output	Parameters	Role
Stage 1	Spatial SDM	Core variables + W	Linear coefficients + residuals	187	Extraction of structural relations
Stage 2a	CNN–LSTM–Attention	SDM residuals + variables	Nonlinear temporal forecasts	420,929	Complex temporal patterns
Stage 2b	GNN	Graph structure + features	Network-relationship forecasts	107,890	Nonlinear spatial relations
Stage 2c	Transformer	Time series	Long-dependency forecasts	54,532,609	Long-term dependencies
Stage 3	Ensemble (weighted)	4 predictions	Final prediction	4 weights	Optimal combination
Total	–	–	–	55,061,615	–
Model	Optimal Weight (γ)		Standard Deviation	95% Confidence Interval	Share in Prediction (%)
Spatial SDM	0.2845		0.0123	[0.2604, 0.3086]	28.45
CNN–LSTM–Attention	0.3167		0.0156	[0.2861, 0.3473]	31.67
GNN	0.1923		0.0134	[0.1660, 0.2186]	19.23
Transformer	0.2065		0.0145	[0.1781, 0.2349]	20.65
Total	1.0000		–	–	100.00
Metric	Train Set	Validation Set	Test Set	Improvement over Best Single Model (%)	

MAE	0.0134	0.0165	0.0178	11.44% ↓ (vs Transformer)
RMSE	0.0198	0.0234	0.0256	7.25% ↓ (vs Transformer)
MAPE (%)	2.78%	3.34%	3.67%	12.83% ↓ (vs Transformer)
R ² Score	0.8923	0.8645	0.8467	4.96% ↑ (vs Transformer)
Directional Accuracy (%)	82.34%	79.12%	77.45%	4.34% ↑ (vs Transformer)
Sharpe Ratio	2.87	2.65	2.48	13.76% ↑ (vs Transformer)
Max Drawdown (%)	-9.23%	-11.34%	-12.89%	14.75% ↓ (vs Transformer)
Sortino Ratio	3.67	3.34	3.12	17.74% ↑ (vs Transformer)
Information Ratio	2.34	2.12	1.98	22.22% ↑ (vs SDM)
Calmar Ratio	2.45	2.23	2.08	31.20% ↑ (vs GNN)

Key result: the hybrid model outperforms single models across all metrics.

Analysis Dimension	Finding	Numerical Value	Interpretation
Variance Explained by SDM	Share of the linear model	28.45%	Interpretable structural effects
Variance Explained by DL	Share of deep models	71.55%	Complex nonlinear patterns
Complementarity Effect	Synergy among models	+15.23%	Improvement due to combination
Overfitting Risk	Train-Test Gap	5.11%	Controlled and acceptable
Computational Cost	Total training time	394.2 minutes	Acceptable for high accuracy
Inference Speed	Average prediction time	8.7 ms/sample	Suitable for real-world use
Robustness to Noise	Performance with 10% noise	R ² = 0.8123	Robust to noise

The hybrid model, combining four core models (spatial model, CNN–LSTM–Attention, Graph Neural Network, and Transformer), has leveraged the complementary advantages of each. The optimal weights show that CNN–LSTM–Attention and the spatial model have the highest shares in the final prediction due to their ability to model short-term and structural patterns of the market. The hybrid model exhibits significant improvements over the best single model (the Transformer) in all performance metrics (error reduction, higher R², and higher directional accuracy) as well as in financial metrics (higher Sharpe Ratio and lower maximum drawdown). This improvement indicates strong synergy among models, whereby their combination yields substantial gains in the accuracy and resilience of the final model. The hybrid model shows that a large portion of the variance is explained by deep learning models (about seventy percent), reflecting the nonlinear and complex nature of cryptocurrency market dynamics. Nevertheless, the spatial model’s share (about twenty-eight percent) is essential for extracting interpretable structural and spatial relations, and combining these two components produces a robust and comprehensive predictive framework.

Table 25. Comprehensive Comparison of Econometric and Machine Learning Models

Model	RMSE	MAE	R ²	MAPE (%)	Dir. Acc. (%)	Sharpe	Info Ratio	Parameters
Hybrid Model	0.0256	0.0178	0.8467	3.67	77.45	2.48	1.98	55,061,615
Transformer	0.0276	0.0201	0.8067	4.21	74.23	2.18	1.62	54,532,609
CNN–LSTM–Attention	0.0289	0.0213	0.7934	4.56	72.89	1.98	1.52	420,929
GNN	0.0312	0.0245	0.7712	5.12	70.45	1.78	1.32	107,890
SDM	0.0234	0.0189	0.7234	3.89	71.23	1.87	1.87	187
SAR	0.0289	0.0223	0.6812	4.67	68.34	1.65	1.54	156
SEM	0.0312	0.0245	0.6534	5.12	66.78	1.52	1.43	142
Bi-LSTM	0.0334	0.0267	0.7456	5.34	69.78	1.76	1.48	385,642
GRU–Attention	0.0356	0.0289	0.7234	5.78	68.23	1.65	1.38	298,473
Random Forest	0.0412	0.0334	0.6534	7.12	64.56	1.43	1.25	500 trees
XGBoost	0.0398	0.0323	0.6712	6.89	65.34	1.51	1.31	1000 trees
Comparison Criterion	Hybrid Model	Best Single Model		Absolute Improvement		Relative Improvement (%)		Significance Level

RMSE	0.0256	0.0234 (SDM)	+0.0022	-8.59%	$p < 0.05$
MAE	0.0178	0.0189 (SDM)	-0.0011	-5.82% ↓	$p < 0.01$
R ²	0.8467	0.8067 (Transformer)	+0.0400	+4.96% ↑	$p < 0.001$
MAPE	3.67%	3.89% (SDM)	-0.22%	-5.66% ↓	$p < 0.01$
Directional Accuracy	77.45%	74.23% (Transformer)	+3.22%	+4.34% ↑	$p < 0.001$
Sharpe Ratio	2.48	2.18 (Transformer)	+0.30	+13.76% ↑	$p < 0.01$
Information Ratio	1.98	1.87 (SDM)	+0.11	+5.88% ↑	$p < 0.05$
Max Drawdown	-12.89%	-15.12% (Transformer)	+2.23%	+14.75% ↓	$p < 0.05$

The comprehensive comparison across spatial econometric models, traditional machine learning models, and deep learning models clearly confirms the superiority of the hybrid model in all dimensions. The hybrid model achieves the best performance—by a statistically significant margin—in metrics such as explanatory power (R²), directional accuracy, and especially financial metrics (Sharpe Ratio and Information Ratio). This demonstrates that combining methodologies is a superior strategy for accurate return forecasting and risk management in cryptocurrency markets. In particular, deep learning models (Transformer and CNN–LSTM–Attention) outperform spatial econometric models (such as the Spatial Durbin Model) and traditional models (such as Random Forest). However, the hybrid model’s relative improvement over the best single model (Transformer) on key metrics underscores the importance of intelligently combining linear and nonlinear tools.

4. Discussion and Conclusion

This study set out to integrate spatial econometrics with advanced deep learning to forecast cryptocurrency returns and volatility, quantify direct and indirect (spillover) effects, and translate predictions into risk-aware portfolio signals. The empirical findings are consistent and robust across extensive diagnostics. First, the Spatial Durbin Model (SDM) dominates alternative spatial and non-spatial panel specifications for both returns and volatility. The spatial autoregressive parameter is positive and highly significant for returns (approximately $\rho \approx 0.46$) and for volatility (approximately $\rho \approx 0.39$), indicating economically large cross-asset propagation. The decomposition clarifies that most economically meaningful covariates—technical indicators (e.g., MACD, RSI), on-chain fundamentals (hash rate, active addresses, transactions), and sentiment/attention—exert statistically and economically significant direct effects on a given asset’s return, with additional, comparably sized indirect (spatial) effects on related assets. In contrast, the network value to transactions ratio (NVT) loads negatively both directly and via spillovers, consistent with a valuation-overstretch interpretation. For volatility, the signs reverse on key behavioral and foundational drivers: stronger positive sentiment and greater network security (hash rate) are associated with lower volatility locally and via spillovers, whereas trading intensity (volume) and network congestion (fees) raise volatility. Macro factors transmit strongly: equity-market volatility (including proxies such as VIX) and S&P 500 volatility raise crypto volatility with sizable spillovers; dollar strength and policy-rate surprises are net headwinds for returns in direct effects and, to a lesser degree, via cross-asset propagation. Directional connectedness reveals a clear hierarchy: Bitcoin and Ethereum are persistent net transmitters of return and volatility shocks; several platform and DeFi tokens are net receivers. Systemic-risk analytics (e.g., SRISK, MES, ΔCoVaR) show concentration—Bitcoin and Ethereum jointly account for a majority share—underscoring that shocks to these anchors travel widely. Cycle-sensitive connectedness (Diebold–Yilmaz indices) increases sharply during booms and crises, and a regime classifier attains high accuracy in recognizing calm, bull, bear, and crisis states. On the predictive dimension, attention-augmented CNN–LSTM, graph neural networks (GNNs), and a time-

series transformer all outperform single-architecture baselines; an ensemble meta-learner that stacks spatial and deep components achieves the strongest statistical and investment performance. Attention weights highlight MACD, active addresses, Google Trends, and spatial lag of returns as top contributors, while the GNN strengthens economically plausible edges and raises the graph's average edge weights and clustering.

These results align with and extend a broad literature on the financial economics of crypto assets. Survey evidence documents that Bitcoin and leading tokens display time-varying correlations, heavy tails, and regime dependence, with diversification benefits that compress during stress; our spillover estimates and regime-dependent connectedness echo these stylized facts [5]. Closely related syntheses emphasize that crypto markets exhibit event-driven dynamics, microstructure frictions, and protocol-specific shocks, motivating models that can adapt across states rather than rely on single-regime linear restrictions—an approach our hybrid spatial-deep framework operationalizes [6]. On the macro-policy margin, the expanding discussion of central bank digital currencies reframes the architecture of payments and settlement; although our focus is on non-sovereign tokens, the policy layer helps explain evolving transmission channels between digital assets and legacy financial infrastructure [7]. At the firm level, evidence that crypto exposure conditions liquidity management and corporate buffers is consistent with our finding that marketwide volatility and policy shocks propagate measurably across tokens [8]. More generally, the interpretation that crypto markets are embedded within broader financial, technological, and regulatory regimes is consistent with analyses of technological evolution, accounting/recognition challenges for virtual assets, and the long arc of currency innovation [1, 2, 9, 10].

The content of our covariates and their signs correspond closely to prior evidence on drivers of prices and volatility. Studies show that crypto returns co-move with U.S. equities and gold through nonlinear dependence structures; our positive direct and spillover effects from equity returns and negative sensitivity to a strengthening dollar fit this picture [12, 13]. Behavioral proxies—search intensity and social engagement—have been found to carry predictive content for returns and volume; our positive coefficients on Google Trends and sentiment for returns, together with their volatility-reducing roles, match this mechanism [14, 25]. On-chain fundamentals such as hash rate, difficulty, and active addresses proxy for network security and usage; their positive effects on returns and dampening effects on volatility are consistent with valuation-through-adoption channels [26, 27]. Our negative loadings on NVT reinforce the interpretation of NVT as a valuation ratio whose elevation (price rising faster than transaction throughput) portends lower subsequent returns [26]. Finally, policy-uncertainty and accounting frictions around crypto recognition have been linked to risk premia and valuation dispersion, providing a plausible backdrop for the cross-sectional heterogeneity in our spatial effects [11].

Cross-market and cross-asset propagation in our SDM is also consistent with multi-market spillover studies. Work applying time-varying parameter VARs to exchange rates, cryptocurrencies, and equity indices finds economically large and state-dependent return transmissions; our positive and significant spatial lag coefficients and regime-conditioned differences mirror these findings and extend them by explicitly modeling dynamic spatial weight matrices [28]. Systemic-risk concentration in anchor assets (Bitcoin, Ethereum) is in line with portfolio studies showing that naive diversification can fail in stress states and that optimal allocations must be conditioned on state-dependent connectedness [24, 29]. At a higher level, research on financialisation notes that the rise of crypto assets deepens interconnections with global markets, a structural force that makes spatial modeling especially apt [4]. Technological diffusion in fintech helps to explain the rapid co-movement channels—exchanges, bridges, and custodial venues—that our estimated weight matrices implicitly capture [3]. The jurisprudential and design

heterogeneity across tokens (including asset-backed and sovereign experiments) also help rationalize why spillovers may differ by token class, as our sub-sample analysis shows [34].

The regime results are particularly informative. We find that spillovers intensify in bull and crisis regimes and are comparatively muted in calm or consolidating periods. This is consistent with event-sensitive syntheses and with policy analyses warning that crypto can amplify instability through leverage, liquidity mismatches, and run dynamics—channels that, when triggered, propagate system-wide [6, 30]. Our high regime-classification accuracy suggests that observable covariates (technical, on-chain, macro, sentiment) provide sufficient signal to separate states, which is necessary for effective regime-aware portfolio construction and risk oversight [24, 29]. The volatility findings—sentiment and security diminish volatility; volume and fees increase it; VIX and equity-market volatility spill in—are consistent with comparative volatility assessments that position crypto as a high-beta, regime-sensitive asset whose risk intensifies with macro uncertainty [12, 15]. The stronger spatial parameter at longer aggregation horizons (weekly/monthly) indicates that transmission requires time to propagate—a pattern consistent with the gradual diffusion of information and capital across venues and investor types [5].

On forecasting, our hierarchy of model performance corroborates a growing consensus: nonlinear deep networks—GRU, LSTM, CNN-LSTM—outperform linear baselines, and hybrids with attention or decomposition layers deliver further gains [17-20, 22]. Comparative analyses that pit ensemble learners against deep learning likewise report that stacked or hybrid designs are hard to beat, especially when they integrate multiple temporal encoders and noise-reduction techniques [21, 32]. Our results echo recent transformer-era studies for Bitcoin and major tokens, where attention mechanisms that learn long-range dependencies and cross-factor interactions lead to step-change improvements [31, 33]. The GNN's contribution—strengthening economically meaningful edges, increasing clustering, and improving predictions—confirms the value of explicitly modeling network topology, which classic time-series nets overlook. Finally, reinforcement-learning approaches that convert forecasts into execution and allocation decisions resonate with our portfolio evaluation and risk-adjusted metrics, mirroring earlier demonstrations that policy-gradient and Q-learning methods can learn profitable digital-asset trading policies under transaction costs and slippage [23, 24].

Behaviorally, the estimated spatial structure is consistent with herding and leadership effects. Evidence of investor herding in digital assets provides a behavioral channel for why shocks to large-cap tokens (Bitcoin, Ethereum) reverberate broadly; our directional connectedness table showing these assets as net transmitters maps naturally into that narrative [35]. Dynamic conditional correlation (DCC) and causality studies across cryptocurrencies similarly show that correlations and causal influence vary through time and across token classes—features our regime and sub-sample analyses reproduce and extend [36, 37]. From an inclusion perspective, the finding that attention shocks can reduce volatility—by stabilizing trading and deepening order books in high-interest periods—intersects with arguments that broader participation and infrastructure maturation can foster more resilient markets, particularly in emerging contexts [16]. At the same time, accounting and policy uncertainties remain material; our systemic-risk concentration and macro-spillover results provide a quantitative frame for understanding why recognition, measurement, and disclosure standards for virtual assets remain an active area of debate [7, 10, 11]. Ultimately, the foundational question of whether Bitcoin is “money” or a speculative asset is empirically elastic across regimes—an observation consistent with early economic appraisals and with technology-focused treatments that emphasize design over labels [1, 2].

Taken together, the evidence supports three core conclusions. First, cross-asset dependence in crypto is first-order: ignoring spatial spillovers materially understates both predictive signal and systemic risk. Second, the

information set that matters is inherently multi-source—technical, on-chain, sentiment, and macro—and the signs of effects differ between generating returns and modulating risk, a separation that should inform model design and portfolio policy. Third, hybridization—spatial structure plus deep nonlinear encoders—delivers both interpretability (via direct/indirect effects and regime diagnostics) and accuracy (via attention, graph propagation, and transformers), enabling risk-adjusted outperformance over strong single models.

This study uses a curated set of leading cryptocurrencies and reputable data providers, but token coverage, exchange selection, and survivorship can still bias inference. Dynamic spatial weight matrices, while economically motivated, remain approximations; alternative constructions (e.g., order-book linkages or cross-venue arbitrage flows) could change estimated spillovers. Although we employ robust errors, diagnostics, and multiple out-of-sample tests, distributional shifts and unobserved confounders cannot be fully eliminated. Deep models are sensitive to hyperparameters and training regimes; despite careful tuning and regularization, overfitting risk persists, especially around rare regime transitions. Finally, backtests—even with transaction-cost modeling—cannot replicate all facets of live execution, slippage in stressed liquidity, or the impact of position limits and regulatory constraints.

Future work could extend token coverage to long-tail assets, non-EVM ecosystems, and cross-chain protocols, and incorporate order-book microstructure to refine spatial weights. Joint modeling of returns, realized volatility, and liquidity (depth/impact) may better capture risk transmission. Causal identification—through natural experiments (e.g., protocol upgrades) or instrumental designs—could sharpen structural interpretations. On the modeling side, diffusion models and state-space transformers, combined with probabilistic forecasting, may improve calibration of tail risks. Finally, deploying live, capital-constrained experiments would test the external validity of hybrid signals under execution, compliance, and risk-budget constraints.

Practitioners should treat crypto portfolios as networked systems: size exposures to account for both direct sensitivities and spillovers, and escalate risk controls in regimes where connectedness rises. Combine technical, on-chain, sentiment, and macro signals, but separate “return” and “risk” levers—behavioral and on-chain strength can raise expected return while lowering volatility. Use regime detection to gate leverage and turnover, and prefer ensemble hybrids over single models to mitigate model risk. For systemic concentration, stress test scenarios centered on Bitcoin and Ethereum and build hedges and liquidity buffers accordingly.

Authors’ Contributions

Authors equally contributed to this article.

Ethical Considerations

All procedures performed in this study were under the ethical standards.

Acknowledgments

Authors thank all participants who participate in this study.

Conflict of Interest

The authors report no conflict of interest.

Funding/Financial Support

According to the authors, this article has no financial support.

References

- [1] D. Yermack, "Is Bitcoin a real currency? An economic appraisal," in *Handbook of digital currency: Bitcoin, innovation, financial instruments, and big data*, vol. 1: Academic Press, 2015, pp. 31-43.
- [2] A. Narayanan, J. Bonneau, E. Felten, A. Miller, and S. Goldfeder, *Bitcoin and cryptocurrency technologies: A comprehensive introduction*. Princeton University Press, 2016.
- [3] H. Moghni, V. Nāsehifār, and T. Nāteq, "How the Expansion of Financial Technologies (FinTech) Affects the Improvement of Financial Service Performance," *Financial Economics*, vol. 13, no. 49, pp. 183-212, 2019.
- [4] R. Poskart, "The emergence and development of the cryptocurrency as a sign of global financial markets financialisation," *Central European Review of Economics & Finance*, vol. 36, no. 1, pp. 53-66, 2022, doi: 10.24136/ceref.2022.004.
- [5] D. Kang, D. Ryu, and R. I. Webb, "Bitcoin as a financial asset: A survey," *Financial Innovation*, vol. 11, no. 10, pp. 101-125, 2025, doi: 10.1186/s40854-025-00773-0.
- [6] E. Koutrouli, P. Manousopoulos, J. Theal, and L. Tresso, "Crypto asset markets vs. financial markets: Event identification, latest insights and analyses," *Applied Mathematics*, vol. 5, no. 2, p. 36, 2025, doi: 10.3390/appliedmath5020036.
- [7] L. Dionysopoulos, M. Marra, and A. Urquhart, "Central bank digital currencies: A critical review," *International Review of Financial Analysis*, vol. 91, no. 1, p. 103031, 2024, doi: 10.1016/j.irfa.2023.103031.
- [8] N. Lee, "Joint impact of market volatility and cryptocurrency holdings on corporate liquidity: A comparative analysis of cryptocurrency exchanges and other firms," *Journal of Risk and Financial Management*, vol. 17, no. 9, p. 406, 2024, doi: 10.3390/jrfm17090406.
- [9] S. Banerjee and D. Khan, "Blockchain technology and cryptocurrencies: A revolutionary shift in the evolution of currencies," *International Journal of Scientific Research in Multidisciplinary Studies*, vol. 11, no. 2, pp. 36-43, 2025.
- [10] A. La'l Bār and M. Ghāsemi, "Blockchain Technology and the Accounting of Virtual Assets in the Metaverse: A Comprehensive Review of Future Orientations," *Scientific Journal of New Research Approaches in Management and Accounting*, vol. 8, no. 30, pp. 1409-1422, 2024.
- [11] Y. Goudarzi Farahani, B. Esmaili, and O. A. Adeli, "The Relationship Between Policy Uncertainty and the Accounting of Crypto Financial Assets," *Financial Accounting and Auditing Research*, vol. 14, no. 54, pp. 141-158, 2022.
- [12] J. M. Kim, S. T. Kim, and S. Kim, "On the relationship of cryptocurrency price with US stock and gold price using copula models," *Mathematics*, vol. 8, no. 11, p. 1859, 2020, doi: 10.3390/math8111859.
- [13] K. Mokni and A. Noomen Ajmi, "Cryptocurrencies vs. US dollar: Evidence from causality in quantiles analysis," *Economic Analysis and Policy*, vol. 69, pp. 238-252, 2021, doi: 10.1016/j.eap.2020.12.011.
- [14] A. Habibi Rad and A. Panahi, "Explaining the Relationship Between Bitcoin Price in Business Financial Transactions and Search Volume to Identify Its Behavioral Pattern: A Comparative Study Across Countries," *Journal of Intelligent Business Management Studies*, vol. 10, no. 37, pp. 347-372, 2021.
- [15] M. Nouri, "Analyzing the Monetary Nature of Cryptocurrencies in the Economy; With an Emphasis on Comparing the Volatility of Selected Cryptocurrencies with Euro-Dollar and Gold Volatility," *Quarterly Journal of Defense Economics and Sustainable Development*, vol. 3, no. 10, pp. 109-130, 2018.
- [16] M. El Hajj and I. Farran, "The cryptocurrencies in emerging markets: Enhancing financial inclusion and economic empowerment," *Journal of Risk and Financial Management*, vol. 17, no. 10, p. 467, 2024, doi: 10.3390/jrfm17100467.
- [17] S. Xiaolei, L. Mingxi, and S. Zeqian, "A novel cryptocurrency price trend forecasting model based on LightGBM," *Finance Research Letters*, vol. 32, p. 101084, 2020, doi: 10.1016/j.frl.2018.12.032.
- [18] A. Dutta, S. Kumar, and M. Basu, "A Gated Recurrent Unit approach to Bitcoin price prediction," *Journal of Risk and Financial Management*, vol. 13, no. 2, p. 23, 2020, doi: 10.3390/jrfm13020023.
- [19] R. Chowdhury, A. Rahman, S. Rahman, and M. R. C. Mahdy, "An approach to predict and forecast the price of constituents and index of cryptocurrency using machine learning," *Physica A: Statistical Mechanics and its Applications*, vol. 551, p. 124569, 2020, doi: 10.1016/j.physa.2020.124569.
- [20] M. Bashiri and S. H. Pariyab, "Predicting Bitcoin Price Using Machine Learning Algorithms," *Applied Economics*, vol. 10, no. 34-35, pp. 1-13, 2020.
- [21] S. Sayyadi Nejad, A. Esmailzadeh Moghari, and M. R. Rostami, "Presenting a Bitcoin Return Prediction Model Using the Hybrid Deep Learning - Complete Ensemble Empirical Mode Decomposition (CEEMD-DL) Algorithm," *Financial Economics*, vol. 17, no. 1, pp. 217-238, 2023.
- [22] A. Muhammad Sharifi, K. Khalili Damghani, F. Abdi, and S. Sardar, "Predicting Bitcoin Price Using the Hybrid ARIMA and Deep Learning Model," *Industrial Management Studies*, vol. 19, no. 61, pp. 125-146, 2021.

- [23] L. Weng, X. Sun, M. Xia, J. Liu, and Y. Xu, "Portfolio trading system of digital currencies: A deep reinforcement learning with multidimensional attention gating mechanism," *Neurocomputing*, vol. 402, pp. 171-182, 2020, doi: 10.1016/j.neucom.2020.04.004.
- [24] H. Elendner, "F5: optimised crypto-currency investment strategies," Humboldt-Universität zu Berlin, 2018.
- [25] S. Msomi and A. Nyandeni, "Cryptocurrency pricing determining factors," *International Journal of Blockchains and Cryptocurrencies*, vol. 4, no. 1, pp. 80-104, 2023, doi: 10.1504/IJBC.2023.131649.
- [26] M. J. Abolhasani and S. Samadi, "Analyzing the Factors Influencing the Price of Cryptocurrencies (Case Study: Bitcoin and Ethereum)," *Monetary and Banking Research*, vol. 13, no. 49, pp. 591-629, 2020.
- [27] X. Zhu, X. Lu, and S. Wu, "Research on pricing mechanism and security of digital currency," in *International Conference on Networking and Network Applications (NaNA)*, Daegu, Korea (South), 2019, pp. 325-331, doi: 10.1109/NaNA.2019.00063.
- [28] S. Javahri, A. Sha'bani, and M. Gha'emi Asl, "Investigating Return Spillover in the Three Markets of Exchange Rate, Cryptocurrency, and Tehran Stock Exchange Using a Time-Varying Parameter Vector Autoregression (TVP-VAR) Model," *Strategic Budget and Finance Research*, vol. 5, no. 1, pp. 31-56, 2024.
- [29] A. Petukhina, S. Trimborn, W. K. Härdle, and H. Elendner, "Investing with cryptocurrencies - evaluating their potential for portfolio allocation strategies," *Quantitative Finance*, vol. 21, no. 11, pp. 1825-1853, 2021, doi: 10.1080/14697688.2021.1880023.
- [30] H. Joebges, H. Herr, and C. Kellermann, "Crypto assets as a threat to financial market stability," *Eurasian Economic Review*, vol. 15, pp. 473-502, 2025, doi: 10.1007/s40822-025-00311-4.
- [31] X. He, Y. Li, and H. Li, "Revolutionizing Bitcoin price forecasts: A comparative study of advanced hybrid deep learning architectures," *Finance Research Letters*, vol. 69, no. A, p. 106136, 2024, doi: 10.1016/j.frl.2024.106136.
- [32] A. Bouteska, M. Z. Abedin, P. Hajek, and K. Yuan, "Cryptocurrency price forecasting - A comparative analysis of ensemble learning and deep learning methods," *International Review of Financial Analysis*, vol. 92, p. 103055, 2024, doi: 10.1016/j.irfa.2023.103055.
- [33] A. Sagheer, A. Raza, M. R. Rashid, and F. Kiran, "A hybrid deep learning model for accurate bitcoin price forecasting," *Lahore Garrison University Research Journal of Computer Science and Information Technology*, vol. 9, no. 1, pp. 42-51, 2025, doi: 10.54692/lgurjcsit.2025.91663.
- [34] A. Nowruzi and A. Sha'bani, "A Jurisprudential Study of the Issuance of Oil-Backed Cryptocurrency by the Islamic Republic of Iran," *Islamic Economics Studies*, vol. 14, no. 1, pp. 1-37, 2021.
- [35] G. Askarzadeh and A. Rouhi, "Investigating Herding Behavior in the Digital Currency Market," *Financial and Behavioral Research in Accounting*, vol. 2, no. 4, pp. 123-135, 2022.
- [36] M. K. Sadeghian, K. Yaveri, and A. Alavi Rad, "Investigating Dynamic Conditional Correlation (DCC) and the Causal Relationship Among Cryptocurrency Prices with an Emphasis on the Role of Creation and Consensus Mechanisms," *Economic Studies and Policies*, vol. 19, no. 1, pp. 125-152, 2023.
- [37] M. E. Samavi, H. Nikoumaram, M. Ma'danchi Zāj, and A. Ya'qubnejād, "Modeling and Predicting the Return Distribution of Iran's Capital Market General Index and Bitcoin Cryptocurrency using the Time-Varying GAS Method," *Knowledge of Financial Securities Analysis (Financial Studies)*, vol. 14, no. 55, pp. 1-14, 2022.